

A COMPARISON OF TWO RAIN-ON-SNOW EVENTS AND THE SUBSEQUENT HYDROLOGIC RESPONSES IN THREE SMALL RIVER BASINS IN CENTRAL PENNSYLVANIA

*Scott Kroczyński
NOAA/National Weather Service, Middle Atlantic River Forecast Center,
State College, PA*

ABSTRACT

Unusually deep snowpacks existed across portions of central Pennsylvania during both January 1978 and January 1996. Significant rain fell on top of both of these snowpacks, yet the hydrologic responses that resulted from the two rain-on-snow events were drastically different. A comparison of the two events, and the antecedent hydrometeorological conditions leading up to them, was made to gain insight into what caused the varied hydrologic responses. The scope of the comparison was three small adjoining subbasins located in the upper portions of central Pennsylvania's Juniata River basin, a significant tributary to the lower Susquehanna River. The output from the snow model portion of a hydrologic model was also compared for each of the two events. Results from the research indicate that the most critical factors in determining the magnitude of the hydrologic responses were snowpack conditioning and subsequent melting preceding the arrival of heavy rainfall, as well as rainfall intensity and rainfall duration.

1. INTRODUCTION

In January 1978 (J78) and again in January 1996 (J96), unusually deep snowpacks existed across portions of central Pennsylvania. A significant rain fell upon both of these snowpacks. The resulting hydrologic response in J78 was relatively minor with no flooding, while in contrast the greatest midwinter flood in modern Pennsylvania history occurred in J96. A comparison of these two apparently similar situations, and their subsequent dissimilar outcomes, would benefit operational hydrometeorologists faced with similar

situations in the future. Why did a major widespread flood event occur in J96, while no flooding occurred in J78? The primary purpose of this investigation is to attempt to answer this question for three small adjoining subbasins located in the upper portions of the Juniata River basin in central Pennsylvania (Figs. 1 and 2). Identifying those factors critical in determining the magnitude of past hydrologic responses can benefit operational hydrometeorologists faced with similar situations in the future. Any insight that provides for the early recognition and accurate prediction of those relatively rare weather and flood events that

are truly life-threatening and property-damaging is valuable.

2. BACKGROUND

Much has already been written about the causes and impacts of the J96 flood event. A broad evaluation of the event was provided by Anderson and Larson (1996). Meanwhile, Yarnal et al. (1997) published a regional analysis of the event for the Susquehanna River basin. On a local scale, Leathers et al. (1998) described in detail the causes of the flooding in two of the hardest hit basins located in north-central Pennsylvania, while Barros and Kuligowski (1998) investigated the critical role played by orography. Similarly, the 25-26 January 1978 storm was itself a phenomenal event that occurred in an extremely active winter. Salmon and Smith (1980) provided an excellent synoptic analysis of this “blizzard” that pummeled portions of the Midwest and Northeast with heavy snow, heavy rain and hurricane-force wind gusts¹. But little exists in the literature in the way of comparing two similar and yet extraordinary midwinter scenarios that were acted upon by two similar and yet extraordinary meteorological events, only to produce two drastically different hydrologic responses. A broader, related study was published by Marosi and Pryor (2000) which compares above-average snowfall seasons to the occurrence of wintertime and springtime flooding in the Susquehanna River basin for the past 70 years.

In this investigation, for each of the

two midwinter scenarios a *catalyst meteorological event* was identified, defined simply as a significant rain event that fell upon the existing deep snowpack across the three adjoining subbasins. Identifying these catalyst events allowed for a more effective comparison of antecedent conditions in the months, weeks and days preceding them. In J96, it was the weather event of the 18th - 19th that acted as a catalyst by initiating a severe hydrologic response in the form of a major flood event. Meanwhile, in J78 the weather event of 25th - 26th ***could have, but did not*** initiate a significant hydrologic response. With catalyst events determined, antecedent conditions prior to the onset of significant rainfall are examined, followed by an evaluation of the meteorological conditions associated with the actual catalyst events. A comparison is then made of the hydrologic responses, including a brief assessment of the output from the snow model portion of the National Weather Service River Forecast System (NWSRFS), the suite of hydrologic models used operationally at the Middle Atlantic River Forecast Center (MARFC) and other National Oceanic and Atmospheric Administration (NOAA) National Weather Service (NWS) river forecast centers.

This investigation illustrates that winter/spring river flooding is not effectively predicted simply by knowing (even with great confidence) that heavy rain will fall on top of an existing deep snowpack. Instead, much more subtle factors appear to be critical in determining the magnitude of cold-season hydrologic responses. Other research has shown that during extended periods of snowmelt the sensible and latent heat fluxes into a snowpack are by far the two processes that result in the greatest snowpack conditioning (or ripening) and subsequent melting

¹ The 25-26 January 1978 storm, sometimes referred to as the “Cleveland Superbomb” (Burrows et al. 1979; Salmon and Smith 1980; Gaza and Bosart 1990) should not be confused with the 19-21 January 1978 Northeast Coast snowstorm, as described by Kocin and Uccellini (1990).

(Leathers et al. 1998). The key meteorological factors that increase both sensible and latent heat fluxes into a snowpack are stronger surface wind speeds, higher surface air temperatures and higher surface dewpoint temperatures (Leathers et al. 1998). This study confirms those previous findings and presents additional recommendations that should be useful to operational hydrometeorologists.

3. COMPARISON OF ANTECEDENT CONDITIONS

The study area consists of three small adjoining subbasins located in central Pennsylvania (Fig. 1). The study area is comprised of mainly forested ridges alternating with mainly agricultural valleys, with elevations generally in the range of 240-640 m (800-2100 ft). Three stream gages², each corresponding to an official NWS MARFC forecast point, are located in the combined subbasin area (Fig. 2). These three gages define the drainages of the three adjoining subbasins. The drainage areas of the two upstream subbasins are 518-777 km² (200-300 mi²) in size, while the drainage area of the third downstream subbasin includes the combined drainages of the other two and totals slightly over 2072 km² (800 mi²). Operationally, the three forecast points are all headwater-type forecast points, meaning each is treated independently of the other and no routing of water occurs from one to the next. Due to the relatively small size of the basins and the closeness of the

forecast points (i.e., fast travel time), little would be gained operationally by routing water. Hydrologic responses measured at these three gages/forecast points are compared later in Section 5. Six locations were chosen in and near the study area to compare hydrometeorological data to help analyze antecedent conditions across the combined drainage area preceding each of the two significant rain events (Fig. 2). Locations were selected based mainly on the availability of data, so that a viable comparison could be made.

The first level of comparison makes use of the Climatic Divisions (CDs) developed and used by the NOAA National Climatic Data Center (NCDC) to average data over larger areas considered to have similar climates. A map delineating the 10 CDs used by NCDC for the state of Pennsylvania is superimposed on a map showing the study area used in this paper (Fig. 3). This figure shows that the study area falls entirely within two NCDC Climatic Divisions: CD-7 (Central Mountains), and CD-8 (South-Central Mountains).

For the three months preceding the J78 and J96 rain events (October-December 1977 and 1995, respectively), observed cumulative precipitation was combined and then averaged across CD-7 and CD-8 (Fig. 4) and then compared to 30-year average data. Figure 4 shows that the three-month periods (October-December) in both 1977 and 1995 were somewhat wet compared to normal. The observed cumulative precipitation over the three-month period in 1977 was 29.9 cm (11.8 inches) compared to a 30-year average (October-December) cumulative precipitation of 24.1 cm (9.5 inches), which is about 24% above average. Meanwhile, the same calculation performed with the 1995 data yields an observed

² The United States Geological Survey (USGS) in cooperation with the United States Army Corps of Engineers, the NWS, and other federal and state organizations, owns, operates and maintains a vast national stream-gaging network. Data from this network are critical to the NWS flood warning program. Refer to USGS Fact Sheet FS-048-01 (April 2001).

cumulative precipitation which is about 31% above average. It is interesting to note from the NCDC data that the precipitation was more evenly distributed in 1977 than in 1995. For example, in 1995 observed precipitation went from much-above average in October to below average in December (i.e., it became progressively *drier* in 1995, and yet there *was* flooding in J96), whereas in 1977 precipitation was above average in all three months (and yet there was *no* flooding in J78).

To infer what impact the three-month cumulative precipitation had on soil conditions across the study area, NCDC historical Palmer Drought data (available online at: <http://www.ncdc.noaa.gov/oa/climate/onlineprod/drought/main.html>) was compared for both CDs 7 and 8 (not shown). These data showed that the December 1977 monthly average Palmer Drought Severity Index (PDSI - for a detailed explanation of this index, go online to: http://www.cpc.ncep.noaa.gov/products/analysis_monitoring/cdus/palmer_drought/wpda_note.txt) values for both CDs 7 and 8 were between 2 and 3 (defined as an “unusual moist spell”). Meanwhile, in December 1995 the monthly average PDSI values for both CDs 7 and 8 were approximately 1 (defined as “near normal”). In fact, the Palmer Drought data indicate that conditions in December of 1977 were wetter (with no flooding in J78) than in December of 1995 (with flooding in J96). This suggests, then, that soil moisture conditions across the study area at the end of 1977 were somewhat more moist than soil conditions at the end of 1995.

Figure 5 shows that both three-month periods (October-December) in 1977 and 1995 were cooler than average. The three-month average observed temperature

was 4 °C in 1977 compared to a 30-year average temperature (October-December) of 4.5 °C which is 0.5 °C below average. Meanwhile, in 1995 the average observed temperature was 3.4 °C which is 1.1 °C below average. In terms of trends, in 1977 the three-month period went from cool in October to warm in November, then back to cool in December. Meanwhile, in 1995 it was warm in October but quite cold in November and December (i.e., an early start to winter-like conditions in 1995).

Antecedent conditions during J78 and J96 were then compared, up to the beginning of each of the respective catalyst meteorological events. Using NCDC Climatological Data for Pennsylvania, five locations in or near the study area (see Fig. 2) were selected (based on data availability) to compare observed daily precipitation and observed daily maximum temperatures (note that only one of the five stations had both data sets available for both years). Figure 6 indicates that during J78 (thin traces) a significant precipitation (rain) event occurred 7-8 January accompanied by mild temperatures. This event essentially eliminated whatever limited snowpack had developed across the study area during the early winter (Fig. 7). In the wake of the 7-8 January rain event, nearly two weeks of continuous subfreezing temperatures and three significant snow events occurred all before the catalyst meteorological event of 25-26 January 1978. Meanwhile, Figure 6 also indicates that in J96 (thick traces), after a relatively mild start to the month, subfreezing temperatures dominated the study area 3-14 January. Similar to J78, very little snow existed on the ground at the start of J96 (Fig. 7). However, by 8 January 1996 two significant snow events had occurred, with a third lighter snowfall 11-12 January. Then during the last few days

before the catalyst meteorological event of 18-19 January, much milder air moved into the study area with maximum temperatures topping 10 °C (50 °F) at numerous locations. Only very light precipitation accompanied the intrusion of milder air.

Surface data from observation sites indicate that cumulative monthly precipitation was greater prior to the catalyst event in J78 than in J96 (Fig. 6). But after the rain event of 9 January 1978, all of the precipitation that fell prior to the J78 catalyst event was snow (Fig. 7). Much of the study area had 0.6-0.9 meters (2-3 feet) of snow on the ground in J78 (Figure 7 as well as snow-on-ground observations at other nearby locations, not shown) just prior to the catalyst event, which corresponds to 5.0-7.6 cm (2-3 inches) of water equivalent (potential meltwater, assuming “typical” snow-water ratios [Roebber and Bruening 2003]). This compares to about 0.3-0.6 meters (1-2 feet) of snow on the ground in J96 prior to the catalyst event, which *also* contained 5.0-7.6 cm (2-3 inches) of water equivalent (according to the 1998 NOAA Natural Disaster Survey Report). As mentioned, Figure 6 shows that temperatures in J78 were quite cold during the snow accumulation period (10-21 January, 1978). This suggests that the J78 snowpack was also very cold heading into the catalyst meteorological event with little if any degree of *ripening*. Snowpack ripening is synonymous with snowpack warming. A snowpack that is ripening means that the snow’s density is increasing (as is the percentage of liquid water held by the snowpack). A snowpack ripens as a result of several energy processes acting upon it, including the addition of heat from warm overlying air and from the sun. Meanwhile, in contrast to J78, Figure 6 shows that in the days prior to the J96 catalyst event milder

air overspread the study area. Figure 7 shows that snow depth in J96 peaked *several days* before the catalyst event of 18-19 January 1996 (represented by the vertical lines). Meanwhile, snow depth in J78 peaked just *two days* before the catalyst event of J78 (Fig. 7). Certainly these data indicate that by the time significant rain arrived in J96 the snowpack had already compacted, sublimated, and was becoming ripe as a result of the mild air intrusion indicated in the temperature data (see Fig. 6). This snowpack preconditioning was clearly not as pronounced in J78.

Based on the antecedent data, it appears that the river flood potential in J78 was initially similar to the river flood potential in J96, at least up until a few days prior to the onset of the catalyst meteorological events. Then, milder air in J96 did begin to ripen the J96 snowpack, providing the first clue that a significant hydrologic response *could* occur given the right catalyst meteorological event to act upon the ripening snowpack.

4. COMPARISON OF THE TWO CATALYST METEOROLOGICAL EVENTS

At first glance, the two catalyst meteorological events do not appear to be too different. Figures 8-12 (a,c) provide five days of surface pressure charts centered around the two events, while Figures 8-12 (b,d) contain 500 hPa height charts for the same dates and times.

a. 500 hPa Discussion

The J78 500 hPa chart series (23-27 January) begins (Fig. 8b) with a slowly-progressive split-flow regime, with

significant energy in the southwestern U.S. that is mostly cutoff from the main stream of polar westerlies located to the north. With time, the southern stream energy progresses northeastward and begins to be absorbed into the main (northern) stream of polar westerlies (Figs. 9b and 10b). Then, during the 24 hour period between 12 UTC 25 January and 12 UTC 26 January, very rapid phasing of the northern and southern streams occurs over the Ohio Valley region (Figs. 10b and 11b). This phasing results in a temporary, extreme south-southwestward displacement of the deep polar vortex (at 500 hPa) from its more typical midwinter location near or over Baffin Island, Canada (using National Center for Environmental Prediction (NCEP) Reanalysis Data for the period 1979-1998; see http://wesley.wwb.noaa.gov/ncep_data/index.html) to a position over western Ohio. The intense upper-level system was accompanied by an incredibly deep surface low that has since been referred to as the “Cleveland Superbomb” (Burrows et al. 1979; Salmon and Smith 1980; Gaza and Bosart 1990). The closed, phased and stacked system then tracks northeastward toward the Canadian Maritimes (Fig. 12b). The orientation of the upper-level trough goes from noticeably positive tilt at the beginning of the sequence, to neutral or perhaps slightly negative tilt as phasing occurs just to the west of the study area. The trough then punches rapidly through the study area and continues eastward. Ahead of the trough, height rises develop first over the western Atlantic and then over eastern Canada as the two streams phase over the Ohio Valley. This mid/upper level ridge then progresses eastward into the north Atlantic. Over the study area, westerly flow backs to southwesterly then southerly as phasing occurs, then veers quickly back to southwesterly and westerly as the closed,

phased system passes to the northwest and north.

In comparison, the J96 500 hPa chart sequence (16-20 January) shows a fairly zonal flow (Fig. 8d) that buckles in the eastern Pacific/western U.S. (Fig. 9d). A temporary split in the flow occurs, resulting in a significant southern stream shortwave (Fig. 10d). The energy in the southern stream progresses eastward faster than the energy in the northern stream, creating an obvious negative tilt to the partially-phased mid/upper level trough with time. Full phasing of the southern and northern streams into a single, full-latitude (extending from the high latitudes to the tropics), negatively-tilted open trough occurs over the Ohio/Tennessee Valleys (Fig. 11d). The trough then swings rapidly eastward through the study area into New England and Canada (Fig. 12d). Ahead of the trough, 500 hPa heights build over the western Atlantic and lift northeastward into the north Atlantic. The flow over the study area, similar to 1978, backs from westerly to southwesterly to southerly ahead of the trough, then veers sharply back to the southwest and west behind the trough. In comparing the 500 hPa chart sequences for both events, it is observed that the full-latitude, open nature of the J96 trough allows for more extensive southerly flow up through much of the eastern U.S. than does the more circular flow around the J78 closed Ohio Valley vortex. This suggests a feed of air into the study area that is more tropical in nature. Another observation is that the 500 hPa heights associated with the J96 system are overall considerably higher (also implying warmer and potentially more moist air) than those associated with the J78 system. For example, just before the J96 500 hPa trough axis passes through the study area (Fig. 11d), the 500 hPa heights across

the study area are approximately 5580 m (18,300 ft). In contrast, in J78 the 500 hPa heights across the study area are around 5220 m (17,000 ft) just before the trough axis passes (Fig. 11b). Though beyond the scope of this paper, a comparison of the “thickness” of the 1000-500 hPa layer associated with these two events would provide more insight into their respective thermal structures. The greater the distance between the 1000-500 hPa levels in the atmosphere means the greater or higher the “thickness” values are. Higher thickness values indicate warmer, less dense and more buoyant air which is capable of holding more moisture, while lower thickness values indicate colder, denser and heavier air that is less capable of holding moisture.

b. Surface Discussion

The J78 mean sea level pressure (MSLP) charts begin on 23 January with high pressure centered over the central Appalachian Mountains (Fig. 8a). Detailed surface analyses (not shown) indicate that the air mass over the study area is best described as modified arctic air, its modification being somewhat limited by an extensive snow cover following a series of major snowstorms (see Fig. 7). On 24 January the surface high has moved to a position just off the mid-Atlantic coast (Fig. 9a). Surface winds across the study area are light and from the southwest under the influence of the departing high. Meanwhile, a frontal system is located well to the west, through the center of the country. Low pressure forms on this front in the Gulf Coast region early on 25 January, while a fresh arctic cold front plunges southeastward out of Canada into the north-central U.S. (implied in Fig. 10a). As the Gulf Coast low heads northeastward through the Tennessee

and Ohio Valleys later on the 25 January, extremely rapid intensification occurs due in part to the injection of cold, dry arctic air into the system which acts to strengthen the baroclinic zone along the storm track. The result is an exceptionally deep, mature surface storm center (~959 hPa) which is located just west of Cleveland, OH early on 26 January (Fig. 11a). This storm center then continues northeastward into eastern Canada while gradually weakening (Fig. 12a).

With respect to the study area of central Pennsylvania, detailed surface analyses (not shown) indicate that the modified arctic air mass in place at the beginning of the period is quickly scoured out as strong southerly winds develop between the departing high pressure system and the rapidly intensifying storm system approaching from the southwest. This results in maximum temperatures spiking up to 6-8 °C (mid-40s °F) across the study area just prior to cold frontal passage early on 26 January. However, just east of the study area maximum temperatures soar briefly to 12-13 °C (mid-50s °F) or higher in the warm sector of the storm where modified semi-tropical air is advected as far north as New York state. Rainfall accompanies the arrival of the warmer air, with much of the study area receiving 2.5-5.0 cm (1-2 inches) or more during the 24-hour period from early on 25 January to early on 26 January. Following frontal passage, rainfall rapidly diminishes as first continental polar air and eventually modified arctic air sweeps into the study area. By early on 27 January cold, windy and snowy weather exists across the study area in the wake of the historic winter storm, likely quickly terminating any additional runoff from snowmelt.

The J96 MSLP chart sequence beginning on 16 January (Fig 8c) indicates a

stationary front is located over the study area, separating cool air dammed east of the Appalachians from milder air flowing northward from the Gulf Coast states ahead of a weak low pressure system in the Central Plains. Similar to J78 cold arctic high pressure is located in western Canada, with the leading edge of fresh arctic air moving southeastward through the upper Great Lakes early on 17 January (Fig. 9c) as deep low pressure has formed over Colorado. Early on 18 January arctic air is seen plunging southward deep into Texas. The former Colorado storm system has moved northeastward into Wisconsin and weakened some, while a new low pressure wave forms to the south along the arctic front over Arkansas. Across the study area, residual cool air remains dammed along and east of the Appalachians while increasingly moist and warm air flows northward to the west of the Appalachians (Fig. 10c).

The MSLP analysis on the morning of 19 January indicates the arctic front has progressed eastward and is oriented nearly north-to-south from eastern Canada to the eastern Gulf of Mexico (Fig. 11c). At this time, detailed surface analyses (not shown, but refer to Fig. 11c) indicate at least three low pressure centers are analyzed along/near the wavy front, including one along a prefrontal trough lying just to the lee of the central Appalachian Mountains (Barros and Kuligowski 1998). Rather strong south-southeast surface winds are found along the entire eastern seaboard, resulting in modified tropical air being transported as far north as southeastern Canada. Early morning temperatures of 15.5 °C (60 °F) or higher are found as far north as Burlington, VT, with dewpoint temperatures of 10 °C (50 °F) or higher all the way up the East Coast to New England. Across the study area of central Pennsylvania, all evidence of

cool air damming has disappeared. Early morning temperatures are 12-18 °C (50s and 60s °F). The cold front lies just to the west of the study area, and heavy rain is falling over the study area in association with the front. The heavy rain is organized into a rather narrow band that precedes and accompanies the front, and contains pockets of convection. Strong southerly winds prevail, with dewpoint temperatures of 8-10 °C (upper 40s to near 50 °F) across the study area. The last MSLP chart valid early on 20 January shows the cold front well off the East Coast (Fig. 12c). A Canadian high pressure system is centered over southeastern Ohio, and typically cold midwinter temperatures have returned to the study area. As in J78, the return of the cold temperatures resulted in quite a rapid reduction in runoff from snowmelt.

c. Specific Weather Conditions

Figures 13-14 compare specific weather conditions associated with the two catalyst meteorological events in and near the study area. The charts on the left side of Figure 13 show four days of observed daily precipitation at three locations (refer to Fig. 2) for both events. These charts indicate that the magnitude of the rainfall associated with each event was very similar: at all three locations, approximately 5 cm (2 inches) of rain fell. However, as will be discussed later, the distribution and intensity of the rainfall was quite different. The charts on the right side of Figure 13 show four days of observed daily maximum temperatures recorded at three locations for both events. These charts indicate that maximum temperatures were considerably higher (4-6 °C [7-11 °F], on average) during the J96 event (thick traces) than during the

J78 event (thin traces), a critical observation that will also be discussed later.

Figure 14 compares observed surface wind speeds and surface dewpoint temperatures at three-hour intervals for three locations in and near the study area. The wind speed and dewpoint temperature traces in Figure 14 begin when the wind direction data (not shown) and the dewpoint temperature data first indicated that warm advection had begun at the respective location. It should be immediately apparent in Figure 14 that the thick traces representing the J96 event are much *longer* than the thin traces associated with the J78 event. This means that warm-air advection was occurring for a considerably longer period of time in J96 (approximately three days) compared to J78 (about two days). Close inspection of Figure 14 shows that dewpoint temperatures at all three locations were above 0 °C (32 °F) for an average of about 45 hours prior to cold frontal passage (indicated by vertical lines) in J96, whereas in J78 dewpoint temperatures were above 0 °C (32 °F) at all three locations for only about 27 hours prior to cold frontal passage. Likewise, dewpoint temperatures during J96 were above 4.5 °C (40 °F) at all three locations for an average of about 20 hours prior to frontal passage, but during J78 dewpoint temperatures only briefly reached or rose above 4.5 °C (40 °F) for an average of about 2 hours. Similarly, Figure 14 shows that sustained wind speeds prior to frontal passage exceeded 5.4 m s⁻¹ (10 knots) at all three locations for an average of about 17 consecutive hours in J96, compared to only around 7 hours in J78, and exceeded 7.6 m s⁻¹ (15 knots) for an average of about 10 consecutive hours in J96 compared to only about 3 hours in J78.

Clearly, data show that air and dewpoint temperatures preceding and during

the J96 event were warmer and persisted for a much longer period of time than in J78. Similarly, sustained warm advection winds were stronger and lasted longer in J96 than in J78. Other research has shown that higher winds and a warmer, more moist near-surface atmosphere ripens and eventually (given enough time) partially melts an existing deep snowpack (Leathers et al. 1998). It is therefore assumed from these data that snowpack conditioning and melting was much greater preceding and throughout the J96 event than it was with the J78 event.

Figure 15 compares hourly precipitation associated with the two catalyst events at a representative location (Hollidaysburg, PA) within the study area (see Fig. 2). As previously noted, the magnitude of the two rainfall events was quite similar (see left side of Fig. 13). However, Figure 15 shows that the distribution of the rainfall was very different. In the J78 event (thin trace), a total of 4.1 cm (1.60 inches) of rain fell at Hollidaysburg, PA during a total of 27 non-consecutive hours. The maximum hourly rain amount reported at Hollidaysburg during the J78 event was 0.5 cm (0.18 inches). Meanwhile, during the J96 event (thick trace), 4.6 cm (1.80 inches) fell in a total of just six non-consecutive hours (of which 4.3 cm (1.70 inches) fell in just five consecutive hours), with a maximum hourly amount of 1.0 cm (0.40 inches) (twice, in two consecutive hours). Clearly, the rainfall in the J96 event was much greater in intensity and much shorter in duration than in the J78 event, even though the total amounts were similar.

Figure 16 depicts the intensity of the rainfall during the 1996 event. The study area is approximated as a white-colored parallelogram. The four reflectivity images

from the NWS State College, PA Weather Surveillance Doppler Radar (WSR-88D) span a total time period of about 1.5 hours during the morning of 19 January 1996, just as a pre-frontal trough was crossing the study area (refer to Fig. 11c). Maximum reflectivity across the study area exceeded 55 dBZ, which is highly indicative of convection. Indeed, ground reports (and personal observation) confirmed the isolated occurrence of lightning and thunder along with intense rainfall. It should be noted that there was also some bright band contamination (due to the low freezing levels) which likely enhanced the reflectivity returns to some degree.

5. COMPARISON OF THE RESULTING HYDROLOGIC RESPONSES

Figures 17-19 show the hydrologic responses at the three stream gages that define the three small adjoining subbasins that make up the study area (refer to Figure 2). It is obvious from Figures 17-19 that the hydrologic responses that resulted from the J96 storm system were significantly greater than those caused by the J78 storm system.

The Spruce Creek stream gage defines the smallest (570 km^2 [220 mi^2]) of the three subbasins and is located on the Little Juniata River (Fig 2). The crest (or maximum stage height) at this gage reached 4.0 m (13.0 feet) (Durlin and Schaffstall 1997) in J96 compared to a crest of only 1.4 m (4.5 feet) reached in J78 (Fig. 17). The J96 crest of 4.0 m (13.0) feet corresponds to a peak flow of approximately $453 \text{ m}^3 \text{ s}^{-1}$ ($16,000 \text{ ft}^3 \text{ s}^{-1}$ (cfs)) (Durlin and Schaffstall 1997) compared to a peak flow of less than $57 \text{ m}^3 \text{ s}^{-1}$ (2,000 cfs) associated with the 1.4 m (4.5 foot) crest of J78. The 2.4 m (8.0

foot) flood stage at the Spruce Creek gage corresponds to a flood flow of approximately $173 \text{ m}^3 \text{ s}^{-1}$ (6,100 cfs). The J96 event was considered a moderate-major flood at the Spruce Creek gage. Only two times since the gage was installed in 1938 has the stage been higher than it was in January 1996. Once was in June 1972 (Hurricane Agnes) when the crest was estimated at 5.2 m (17.0 feet), and the other was in November 1950 when a crest of 4.8 m (15.8 feet) was estimated.

At the Williamsburg stream gage, which defines a 754 km^2 (291 mi^2) subbasin on the Frankstown Branch of the Juniata River (Fig. 2), the J96 crest was 5.9 m (19.4 feet), with a peak flow of approximately $509 \text{ m}^3 \text{ s}^{-1}$ (18,000 cfs) [Durlin and Schaffstall 1997]. This compares to a crest of only 2.4 m (7.8 feet) and a peak flow of less than $85 \text{ m}^3 \text{ s}^{-1}$ (3,000 cfs) reached in J78 (Fig. 17). The flood stage at Williamsburg is 3.7 m (12.0 feet) which corresponds to a flood flow of approximately $195 \text{ m}^3 \text{ s}^{-1}$ (6,900 cfs). The J96 flood event was determined to be a new record stage at the Williamsburg stream gage, higher than the old record stage estimated at 5.8 m (19.1 feet) in June of 1889.

Finally, at the Huntingdon stream gage on the Juniata River, which encompasses both the Spruce Creek and Williamsburg subbasins and has a drainage area of 2113 km^2 (816 mi^2) (Fig. 2), the J96 crest reached 4.9 m (15.9 feet) with a peak flow of approximately $1032 \text{ m}^3 \text{ s}^{-1}$ (36,500 cfs) (Durlin and Schaffstall 1997). In comparison the J78 crest was just 2.0 m (6.5 feet) with a peak flow of less than $198 \text{ m}^3 \text{ s}^{-1}$ (7,000 cfs) (Fig. 17). The flood stage at Huntingdon is 3.7 m (12.0 feet), which corresponds to a flood flow of approximately $594 \text{ m}^3 \text{ s}^{-1}$ (21,000 cfs). The January 1996 flood at Huntingdon was the

second highest flood since the gage was installed in 1941. The highest crest was 6.1 m (20.0 feet) reached in June 1972 (Hurricane Agnes).

In all three subbasins, the J96 crests were more than two times higher (or 2.4-3.7 m [8-12 feet]) than the J78 crests in terms of stage, and more than five times greater in terms of peak flow. Flooding in J96 ranged from moderate to record, while no flooding occurred in J78 and in fact the hydrologic responses were less than half bankfull in terms of peak flow. A couple of important observations regarding Figures 17-19 are worth mentioning at this time. The first is that both the J78 and J96 hydrologic responses at all three stream gages were negligible right up until 12-20 hours before the crest (peak flow). Yet, the hydrometeorological data have shown clearly that temperatures were considerably warmer (for several days) preceding the J96 catalyst meteorological event than in J78. The J96 hydrologic response strongly supports the idea that although the J96 snowpack must have been compacting, sublimating and most importantly ripening, any actual melting of the snowpack must have been minimal at least in terms of the snowmelt being sufficient to produce enough runoff to cause the streams to noticeably rise. Another observation is that the stage height at all three locations *preceding* each hydrologic response (or baseflow) was very similar, albeit slightly *higher* in 1978 than in 1996. The reasons for the drastic difference in the magnitude of the two hydrologic responses at the three gages (despite relatively similar hydrometeorological scenarios) are summarized below.

6. SUMMARY

The primary goal of this research was to establish why two apparently similar hydrometeorological scenarios resulted in two quite unique hydrologic responses. Leathers et al. (1998) and Barros and Kuligowski (1998) describe in some detail the causes of the J96 flood event in Pennsylvania. Those authors concluded that a number of hydrometeorological factors occurring in unison caused the severe flooding in Pennsylvania in J96, including: extreme antecedent snow cover; unusually extensive and thick river ice; a powerful synoptic situation that created a deep southerly flow of air which advected unseasonably warm and humid air into Pennsylvania accompanied by strong surface winds; significant snowmelt due to latent and sensible heat processes that were maximized by the high temperatures, dewpoints and surface winds; and unusually intense midwinter rainfall that was strongly orographically enhanced. So how was January 1978 different, and why was there no flooding?

A review of the autumnal (October-December) antecedent conditions preceding each of the two events indicates quite similar conditions across the study area. Precipitation was above normal in both autumns, while temperatures were somewhat below normal during both autumns. The only notable difference is that the precipitation in the autumn of 1977 was more evenly distributed than in the autumn of 1995. In the autumn of 1995, precipitation was heaviest in October, but became progressively lighter in November and December. The drier conditions later in the autumn of 1995 (i.e., closer to the J96 storm) would tend to *lessen* flood potential, rather than increase it. Yet flooding still occurred in J96. This suggests that the autumnal antecedent conditions were not a

critical factor in determining either of the two January hydrologic responses. Then for much of the two-week period preceding each of the two January catalyst meteorological events, hydrometeorological conditions showed some remarkable similarities. For example, the representative snow depth in J78 increased rapidly across the study area from almost zero to nearly 102 cm (40 inches) in the space of about 10 days (Fig 7). Similarly, the representative snow depth in J96 increased rapidly from about zero to nearly 76 cm (30 inches) in about 10 days.

However, a close look at Figure 7 reveals a difference: the snow depth at Altoona, PA in J78 peaked just two days before the beginning of the J78 catalyst meteorological event while in J96 the peak was reached five days before the beginning of the catalyst meteorological event. The fact that the snow depth at Altoona, PA decreased in J96 by over 40 cm (16 inches) (Fig. 7) even before the beginning of the catalyst event suggests that compaction, sublimation, considerable ripening and some melting of the snowpack had already occurred, as supported by observed temperature data (Fig. 6). This snowpack ripening was absent/minimal during J78. In J96 the entire snowpack was already primed to release significant meltwater even *before* the arrival of the catalyst meteorological event and its associated humid, warm, windy and wet weather. In contrast, the J78 snowpack was still very cold and dry at the onset of the catalyst event, suggesting some portion of the energy (sensible and latent heat processes) associated with the event itself had to be spent on just getting the snowpack *ready* (by warming it) to release meltwater.

Table 1 illustrates some of the differences in the two snowpacks by

comparing output generated from a snow model (SNOW-17) used operationally by the NWS. The SNOW-17 model is a conceptual snow accumulation and ablation model that keeps continuous account of several variables needed to describe the state of snow cover (Day 1996; Anderson 1996a, b). The model uses inputs of precipitation and air temperatures to simulate snow conditions, and provides outputs that include estimates of snow water equivalent, areal coverage of snow, and snow cover heat content all for the purpose of computing snowmelt. The upper portion of Table 1 shows SNOW-17 output for the Juniata River at Huntingdon, PA for an eight-day period 20-27 January 1978, while the bottom portion of the table depicts similar output for 15-22 January 1996.

Column 4 of Table 1 shows **Energy Exchange** values generated by the SNOW-17 model for the two time frames. Positive (>0) energy exchange values indicate energy (heat) is entering the cooler snowpack from the relatively warmer atmosphere overlying it, while negative (<0) energy exchange values indicate energy (heat) is leaving the snowpack and entering the relatively cooler atmosphere above it. If heat is entering the snowpack it means that the snowpack is ripening (warming). Still, a snowpack will not actually begin releasing water (melting) until the heat deficit throughout the snowpack can be overcome, or until the mean temperature throughout the snowpack is raised to a temperature of 0 °C (32 °F) or above. Conversely, if heat is exiting the snowpack it means that the snowpack is not ripening and in fact is likely getting colder. Table 1 shows that a maximum energy exchange of +0.27 was reached on 25 January 1978 in association with the J78 event, while a maximum of +0.88 was reached on 19 January 1996 in association

with the J96 event. This means that, at its peak, the heat entering the snowpack in 1996 was more than three times the heat entering the snowpack in 1978³. Moreover, in 1996 there were positive (>0) Energy Exchange values for five days preceding the catalyst event indicating a ripening snowpack, while in 1978 the Energy Exchange values were negative indicating a non-ripening, relatively cold snowpack.

Snowpack warming (ripening) [and to some degree snowmelt, at least enough to moisten the soils] preceding the arrival of significant rainfall appears to be critical in determining the final hydrologic response a particular river basin has when subsequent significant rain falls. If a snowpack is sufficiently warmed it ripens, meaning it is ready to release water (melt). This warming can occur if warm, humid air advects over the snow surface, resulting in latent and sensible heat transfers between the air and the snow surface. Once the mean temperature of the snowpack reaches 0 °C (32 °F), the snow begins to melt, primarily at the top of the snowpack. Since both latent and sensible heat flux are turbulent transfer processes, the greater the wind speeds are at the snow surface, the more efficient the heat transfer will be, resulting in faster ripening and greater subsequent snowmelt. Of course, other non-turbulent processes (such as solar radiation) can also play an important role in ripening and subsequently melting snow, but in J96 other research (Leathers et al. 1998) showed that the turbulent processes were dominant.

Once melting actually begins, the

³ The actual energy exchanges associated with the 1996 event were likely several times higher than indicated in Table 1 (NOAA, 1998). The unusually high winds and dewpoints associated with the 1996 event caused such rare snowmelt rates that the energy exchange values generated by the SNOW-17 model were significantly underestimated.

meltwater first fills the air voids within the snowpack, until the snowpack can no longer hold any more liquid water. Snow, like soil, has a limited capacity to retain liquid water (i.e., snowmelt or rain). The amount of water that snow can hold is typically expressed as a percentage by weight of the solid (ice) portion of the snow (Anderson 1996a, b)⁴. In the absence of rain, the amount of time it takes for the liquid water holding capacity of the snowpack to be satisfied depends on numerous factors, including the depth of the snow and the degree of melting induced by the latent and sensible heat transfer processes. Those processes in turn depend on surface wind speed, surface air temperature, the relative humidity and vapor pressure of the air, and the snow surface temperature. If conditions are such that snowmelt continues, and the liquid water holding capacity of the snowpack is filled, then the excess meltwater finally leaves the snowpack and enters the soil beneath the snow as snowpack outflow. This meltwater in turn first fills the air voids within the soil, until the soil itself can no longer hold any more water. Finally, after the liquid water holding capacities of both the snowpack and the soil have been filled, any excess meltwater becomes surface runoff, which is water that finally reaches the streams and rivers. If a snowpack has been ripening/melting long enough that the snowpack can no longer hold any water and *then* significant rainfall occurs, most if not all of the rainwater essentially passes *directly through* the snowpack. Then, if the flux of water from the rain passing through the snowpack (combined with water from the melting

⁴ For snowpacks in Pennsylvania (and the Northeast in general), the liquid water holding capacity is typically in the range of 5-20 percent (Anderson 1996a, b).

snow) exceeds the infiltration rate of the already moistened soil, a very large percentage of the rainfall is converted directly into surface runoff, which reaches the streams and rivers very quickly, particularly if the rainfall is intense.

In summary, snowpack warming (ripening) and subsequent snowmelt, especially if sustained for a period of 8-12 hours or more (by strong surface winds and the advection of unseasonably warm and moist air), can prime the snowpack and the underlying soils by satisfying the liquid water retaining capacity of each even before the arrival of significant rainfall. Then if significant rain does follow, the rainwater can quickly pass through the wet snowpack to the moist soils beneath and be efficiently and rapidly converted to surface runoff, thereby greatly increasing the magnitude of the hydrologic response. Intense rainfall would result in an even more extreme hydrologic response. For example, 5 cm (2 inches) of rain that fell in just four hours would produce more runoff (faster) than 5 cm (2 inches) spread out over 24 hours. It was this precise scenario that resulted in a major flood across upper portions of the Juniata River Basin in central Pennsylvania (and across a much larger area) during J96. Conversely, in J78 the lack of a sustained period of significant snowpack ripening and melting preceding the rainfall, along with a much less intense and longer duration rain event, resulted in a much more subdued hydrologic response (Figs. 17-19) despite many other similarities with the two scenarios. Simply put, there was just not enough time in J78 for the snowpack to *really get involved*, meaning its contribution to the runoff was minimal.

This investigation shows that the more subtle yet obviously more critical factors in determining the magnitude of a

cold-season hydrologic response appear to be snowpack conditioning (and melting) preceding significant rainfall, and then the duration and intensity of subsequent rainfall. It is concluded from this comparison that a major, widespread midwinter river flood event is likely to occur in Pennsylvania (and presumably elsewhere in the Northeast) when a significant percentage of an above-average snowpack is melted and the resulting runoff is combined with additional runoff produced by a significant rain event. A synoptic meteorological event is necessary to act as a catalyst upon the existing deep snowpack. Such an event should include unusually strong surface winds and unseasonably warm, moist (humid) air at the surface for a sufficient length of time (i.e., on the order of 8-12 hours or more [Fig. 14]). Then, once snowmelt has already begun the addition of widespread significant rainfall, especially if it is abnormally intense for wintertime, will very likely result in major river flooding. In other words, major wintertime river flooding is most likely to occur when a strong storm system more typical of spring (April or May) happens weeks-to-months early and acts upon an existing, above-average, previously ripened (or quickly ripening) snowpack. Finally, if thick, strong and widespread river ice is present as it was in J96, its breakup (caused by the rising water) can in turn cause ice jams to form which can result in locally severe and unpredictable flooding. Also, the large ice floes can be particularly damaging to property. Widespread river ice in general simply complicates and plays havoc with the prediction of crest height and timing as the crest works downstream, due to profound local effects that can occur as a result of the ice breaking up and jamming.

7. OPERATIONAL CONSIDERATIONS FOR PENNSYLVANIA (and the Northeast in general)

The following provides some guidance to assist operational forecasters in the early recognition of increased wintertime river flood potential, and to identify critical factors that convert river flood potential into actual river flooding.

- *An ongoing knowledge of recent antecedent hydrometeorological conditions can be useful in assessing current and future river flood potential.*
- *Widespread significant river flooding is a relatively rare event, and is generally less likely to occur in midwinter than in late winter or early spring (visit www.erh.noaa.gov/er/marfc/Rivers/FloodClimo for flood frequency analyses within the MARFC service area, performed by Chillag and Bleistein).*
- *While above-average seasonal snowfall generally correlates to a higher winter/spring river flood potential (Marosi and Pryor 2000), snowmelt alone without significant rainfall is not likely to cause widespread major river flooding, especially in midwinter. At the same time, significant rainfall on top of a deep snowpack may still not cause river flooding. However, significant widespread rainfall combined with substantial snowmelt will likely lead to potentially serious river flooding.*
- *Snowpack conditioning (ripening) and melting preceding the arrival of significant rainfall are important in determining the magnitude of the hydrologic response. Sensible and latent heat processes can be dominant in ripening and melting snow in the short term. Factors that increase sensible and latent heat fluxes into a snowpack include strong surface winds and unseasonably warm and moist air.*
- *Snowpack ripening and melting increase as cold air damming effects decrease. Therefore, estimating the time of elimination of cold air damming effects (using atmospheric model and sounding data) and tracking (using surface observations) the actual arrival (and subsequent duration) of warm surface air and surface dewpoint temperatures (especially 4.4 °C (40 °F) or higher) is critical in estimating the degree of snowpack ripening and melting.*
- *The “recipe” to convert high river flood potential associated with an existing deep snowpack into actual significant widespread river flooding should include a snowpack that is already quite ripe and has begun melting. Then, a “catalyst meteorological event” is necessary to really aggressively melt (at least partially) the snowpack. The event should provide unseasonably warm surface air and dewpoint temperatures (especially 4.4 °C (40 °F) or higher) and strong surface winds (especially sustained at 4.5-9.0 m s⁻¹ (10-20 mph) or greater)*

blowing from a “warm advection” direction (typically 120-240 degrees), both of which should persist for 8-12 hours or more. Finally, the event should eventually produce widespread significant rainfall (especially mean areal (or basin average) rainfall of 2.5 cm (1 inch) or more). Flooding is likely to be most severe if the rainfall quickly follows a sustained period of snowpack ripening and/or melting and if the rainfall is intense.

- *The breakup of thick (i.e. 15-30 cm (6-12 inches) or more), strong and widespread river ice will generally result in more severe localized river flooding due to ice jams than if river ice was minimal or nonexistent. The breakup of the river ice also complicates the hydrology considerably, and in particular increases the difficulty in accurately predicting the crest heights and timing.*
- *It is very unlikely that a deep snowpack will completely melt in a single event, even under optimum conditions. For this and other reasons, river flood potential may remain high for some time, even after the occurrence of a significant river flood event.*

Acknowledgments. The author wishes to thank Joseph Ostrowski and Ned Pryor of the NWS MARFC for their review of the original manuscript. Mr. David Solano of the NWS MARFC assisted with the graphics. Data sources included the NOAA National Climatic Data Center, the NOAA National Centers for Environmental

Prediction, the NWS Forecast Office at State College, Pennsylvania, the United States Geological Survey (Lemoyne, PA office) and the NWS MARFC.

REFERENCES

- Anderson, E. A., and L. Larson, 1996: The role of snowmelt in the January 1996 floods in the northeastern United States. *Proc. 53d Eastern Snow Conference*, Eastern Snow Conference, Williamsburg, VA, 141-149.
- _____, 1996a: Snow-17 snow model. National Weather Service River Forecast System User's Manual, Part II.2, 24 pp. [Available from NOAA, National Weather Service, Office of Hydrology, SSMC1, 1325 East-West Highway, Silver Spring, MD 20910.]
- _____, 1996b: Snow-17: Initial parameter values for the snow accumulation and ablation model. National Weather Service River Forecast System User's Manual, Part IV.2.2. [Available from NOAA, National Weather Service, Office of Hydrology, SSMC1, 1325 East-West Highway, Silver Spring, MD 20910.]
- Barros, A. P., and R. J. Kuligowski, 1998: Orographic effects during a severe wintertime rainstorm in the Appalachian Mountains. *Mon. Wea. Rev.*, **126**, 2648-2672.
- Burrows, W. R., R. A. Tiedl and R. G. Lawford, 1979: The southern Ontario blizzard of January 26 and 27, 1978. *Atmos. Oceans*, **17**, 306-320.
- Day, G. N., 1996: NWS-43 snow model. National Weather Service River Forecast System User's Manual, Part II.2, 9 pp. [Available from NOAA, National Weather Service, Office of Hydrology, SSMC1, 1325 East-West Highway, Silver Spring, MD 20910.]
- Durlin, R. R., and W. P. Schaffstall, 1997: Water resources data for Pennsylvania, water year 1996, volume 2. U. S. Geological Survey Water-Data Report PA-96-2, 310 pp.

[Available from National Technical Information Service, Springfield, VA 22161.]

- Gaza, R. S., and L. F. Bosart, 1990: Trough-merger characteristics over North America. *Weather and Forecasting*, **5** (No. 2), 314-331.
- Kocin, P. J., and L. W. Uccellini, 1990: *Snowstorms along the northeastern coast of the United States: 1955 to 1985*. *Amer. Meteor. Soc., Meteorological Monographs*, **22** (No. 44), 280 pp.
- Leathers, D. J., D. R. Kluck, and S. Kroczyński, 1998: The severe flooding event of January 1996 across north-central Pennsylvania. *Bull. Amer. Meteor. Soc.*, **79**, 785-797.
- Marosi, W. J., and E. C. Pryor, 2000: Comparison of above average snowfall seasons to the occurrence of winter and springtime flooding in the Susquehanna River basin. NWS Eastern Region Tech. Attach., 2000-1, 5 pp. [Available from NWS Eastern Region Headquarters, Airport Corp. Center, 630 Johnson Ave., Bohemia, NY 11716.]
- National Oceanic and Atmospheric Administration, 1998: Northeast floods of January 1996. NOAA Natural Disaster Survey Report. [Available from NOAA, National Weather Service, Office of Hydrology, SSMC1, 1325 East-West Highway, Silver Spring, MD 20910.]
- Roebber, P. J., and S. L. Bruening, 2003: Improving Snowfall Forecasting by Diagnosing Snow Density. *Weather and Forecasting*, **18**, 264-287.
- Salmon, E. M., and P. J. Smith, 1980: A synoptic analysis of the 25-26 January 1978 blizzard cyclone in the central United States. *Bull. Amer. Meteor. Soc.*, **61**, 453-460.
- Yarnal, B., D. L. Johnson, B. J. Frakes, G. I. Bowles, and P. Pascale, 1997: The flood of '96 and its socioeconomic impacts in the Susquehanna River basin. *J. Amer. Water Resour. Assoc.*, **33**, 1299-1312.

FIGURES

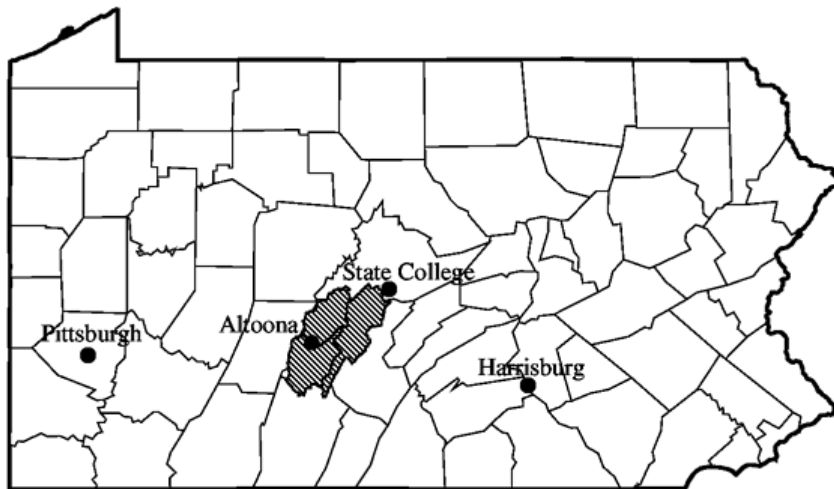


Figure 1. Map of Pennsylvania showing counties and study area (shaded).

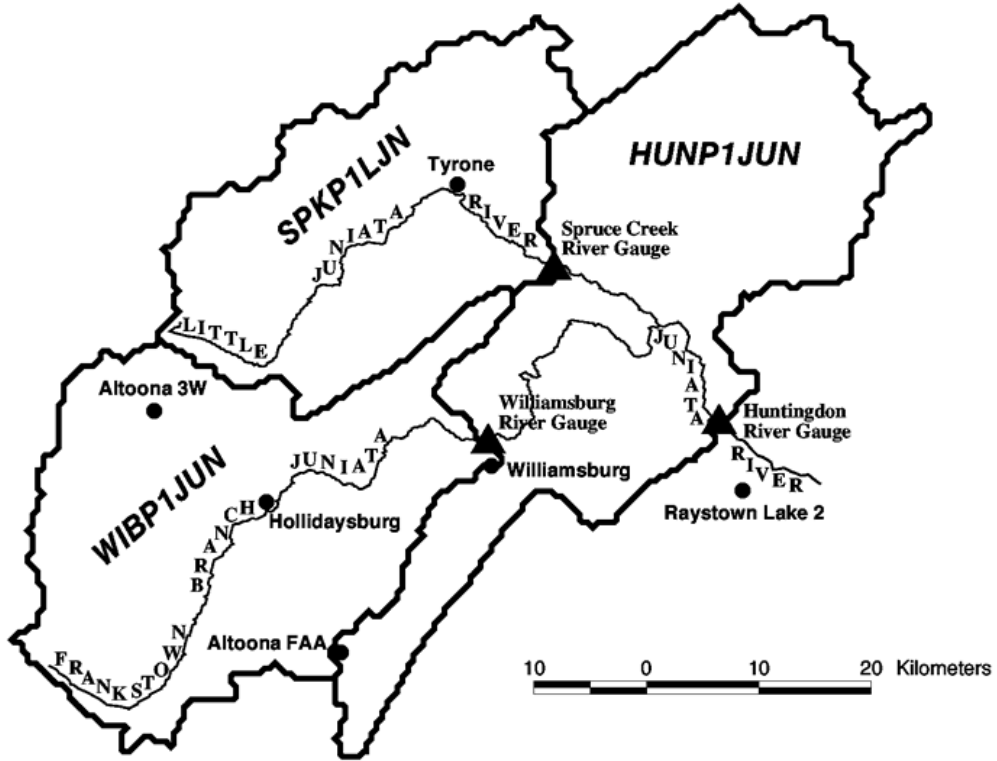


Figure 2. Enlarged map of study area showing locations of stream gages (triangles) and data collection sites (circles).

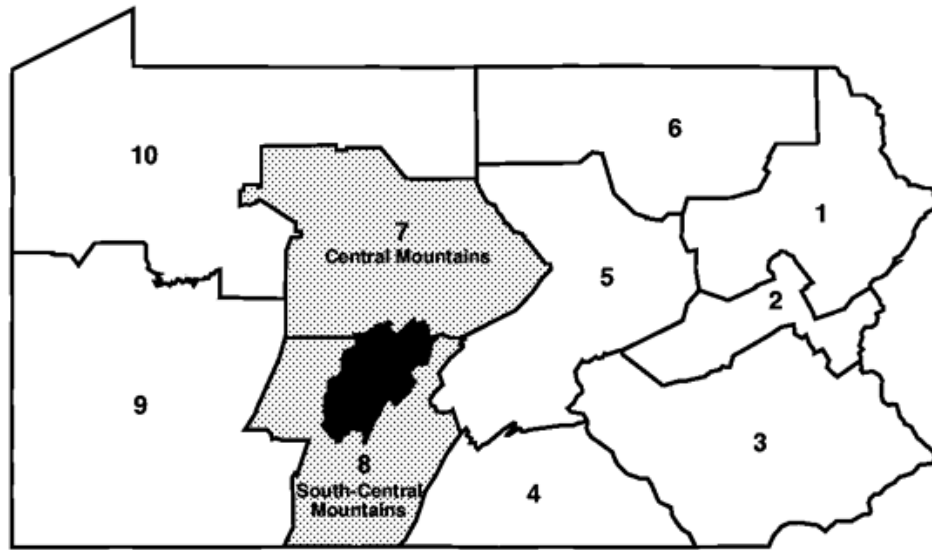


Figure 3. Map of Pennsylvania showing the 10 NCDC Climatic Divisions (CDs). CD 7 and 8 (shaded) encompass the study area (black) and were used for analyses.

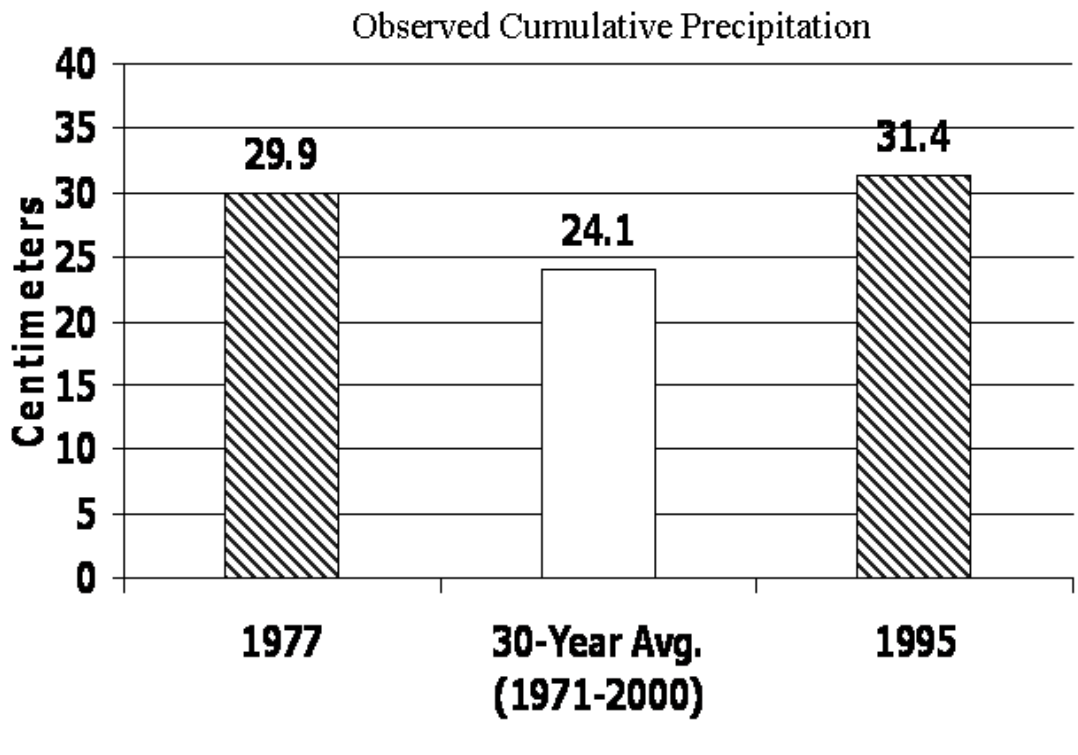


Figure 4. October-December observed cumulative precipitation in centimeters (shaded) during 1977 and 1995 averaged over the two Climatic Divisions that encompass the study area. Thirty year (1971-2000) average cumulative precipitation is also shown (white bar).

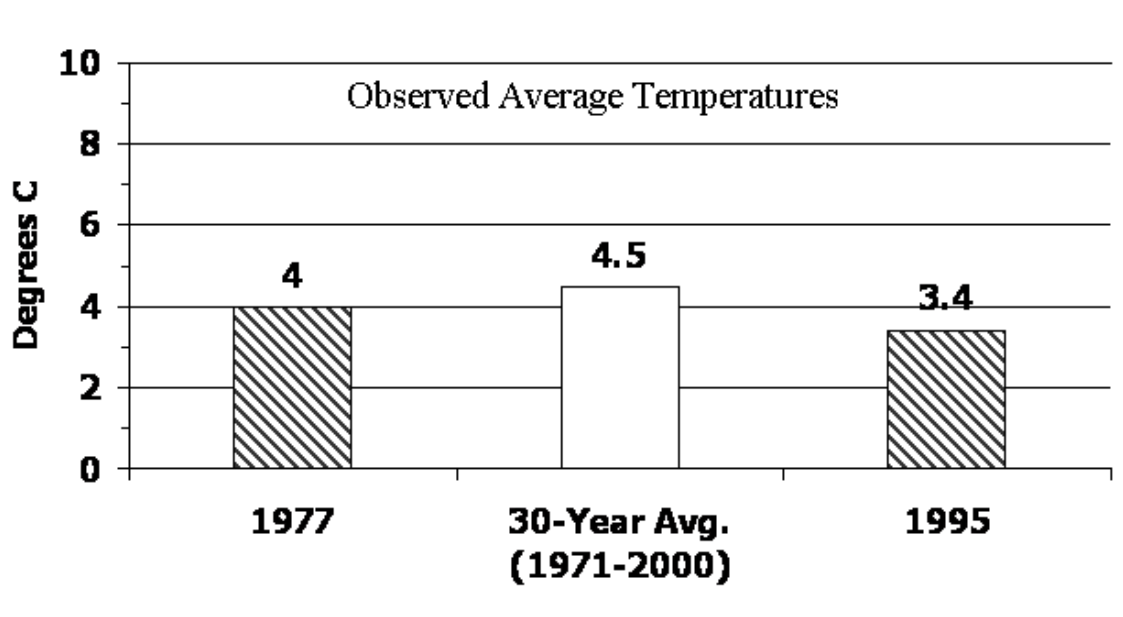


Figure 5. October-December observed average temperatures in °C (shaded bars) during 1977 and 1995 averaged over the two Climatic Divisions that encompass the study area. Thirty-year (1971-2000) average temperatures are also shown (white bar).

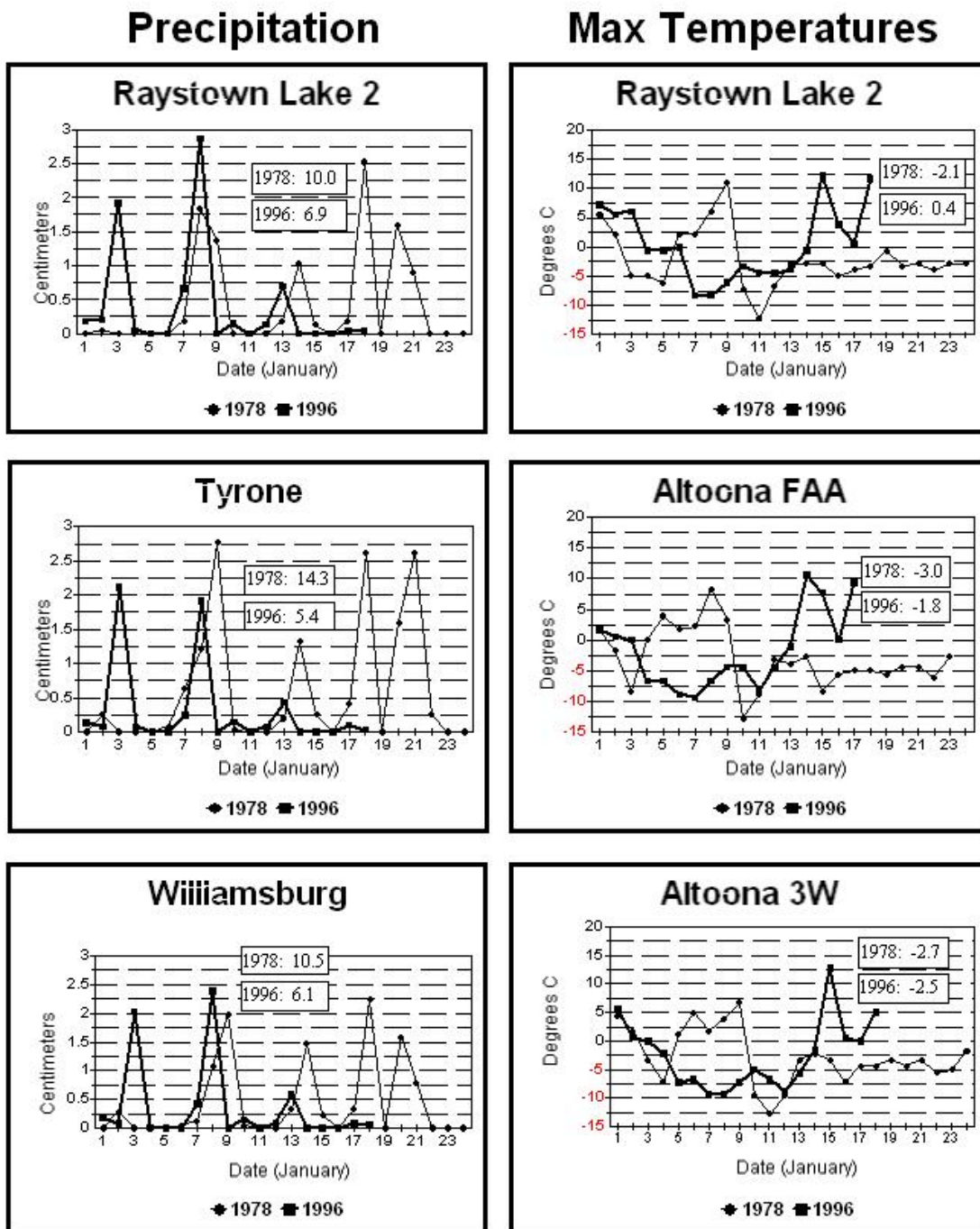


Figure 6. January observed daily precipitation (centimeters) and observed daily maximum temperatures ($^{\circ}\text{C}$) leading up to the catalyst meteorological events of January 1978 (thin trace) and January 1996 (thick trace) for select stations in and near the study area.

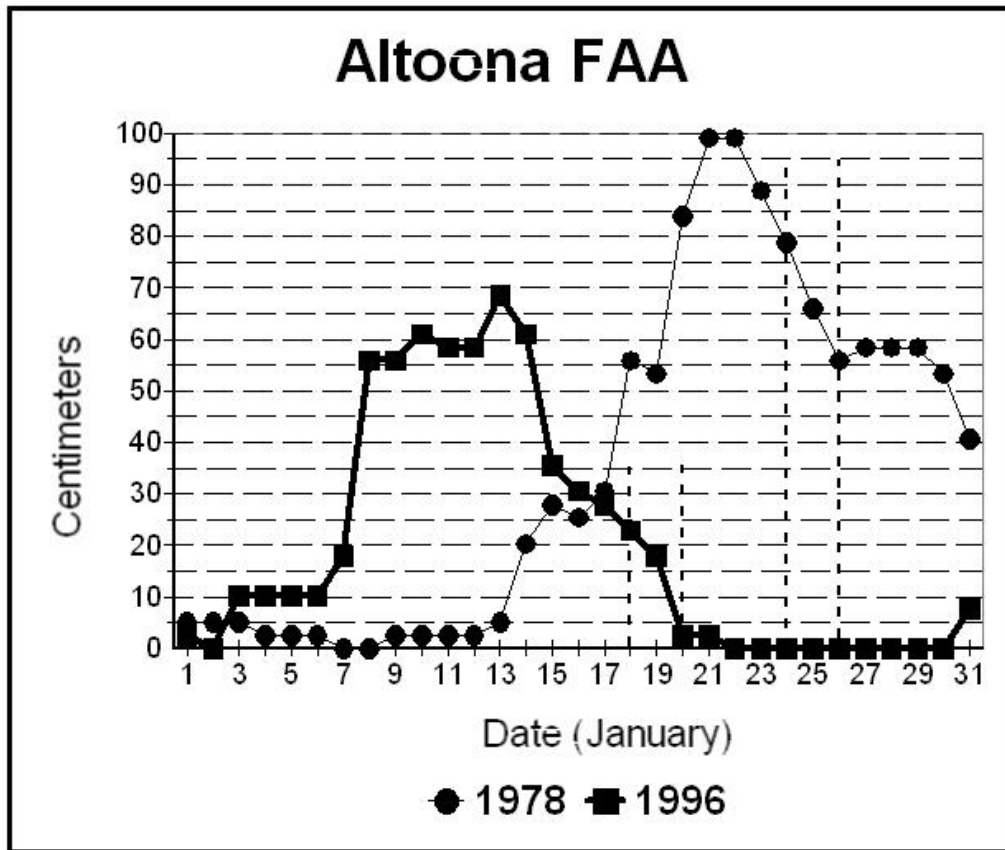


Figure 7. Observed daily snow depth (centimeters) in January 1978 (thin trace) and January 1996 (thick trace) at Altoona, PA. Vertical (dashed) lines indicate the catalyst meteorological events of 25-26 January 1978 and 18-19 January 1996.

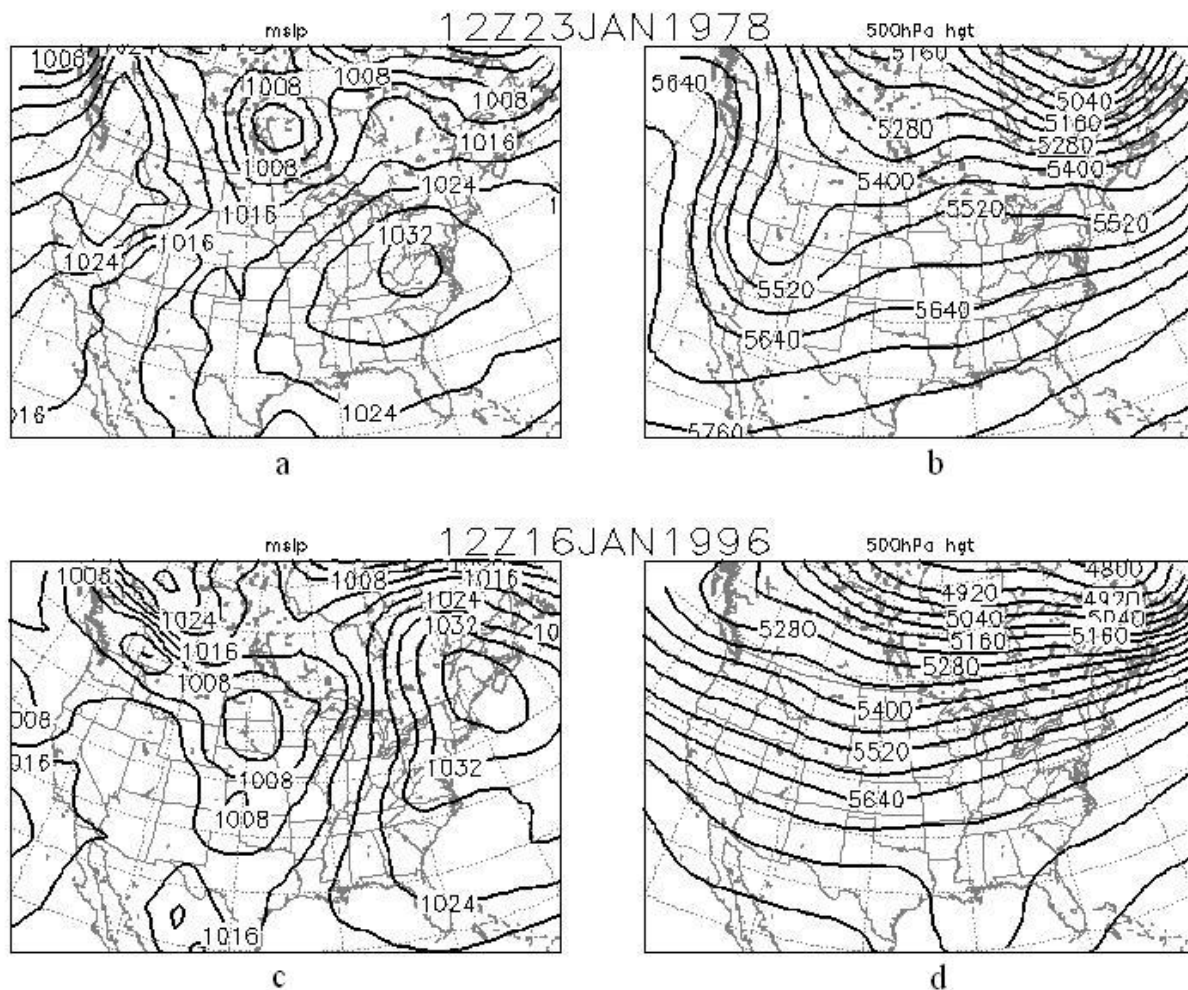


Figure 8. Mean sea level pressure (hPa) and 500 hPa heights (meters) at 12 UTC 23 January 1978 (a,b) and 12 UTC 16 January 1996 (c,d).

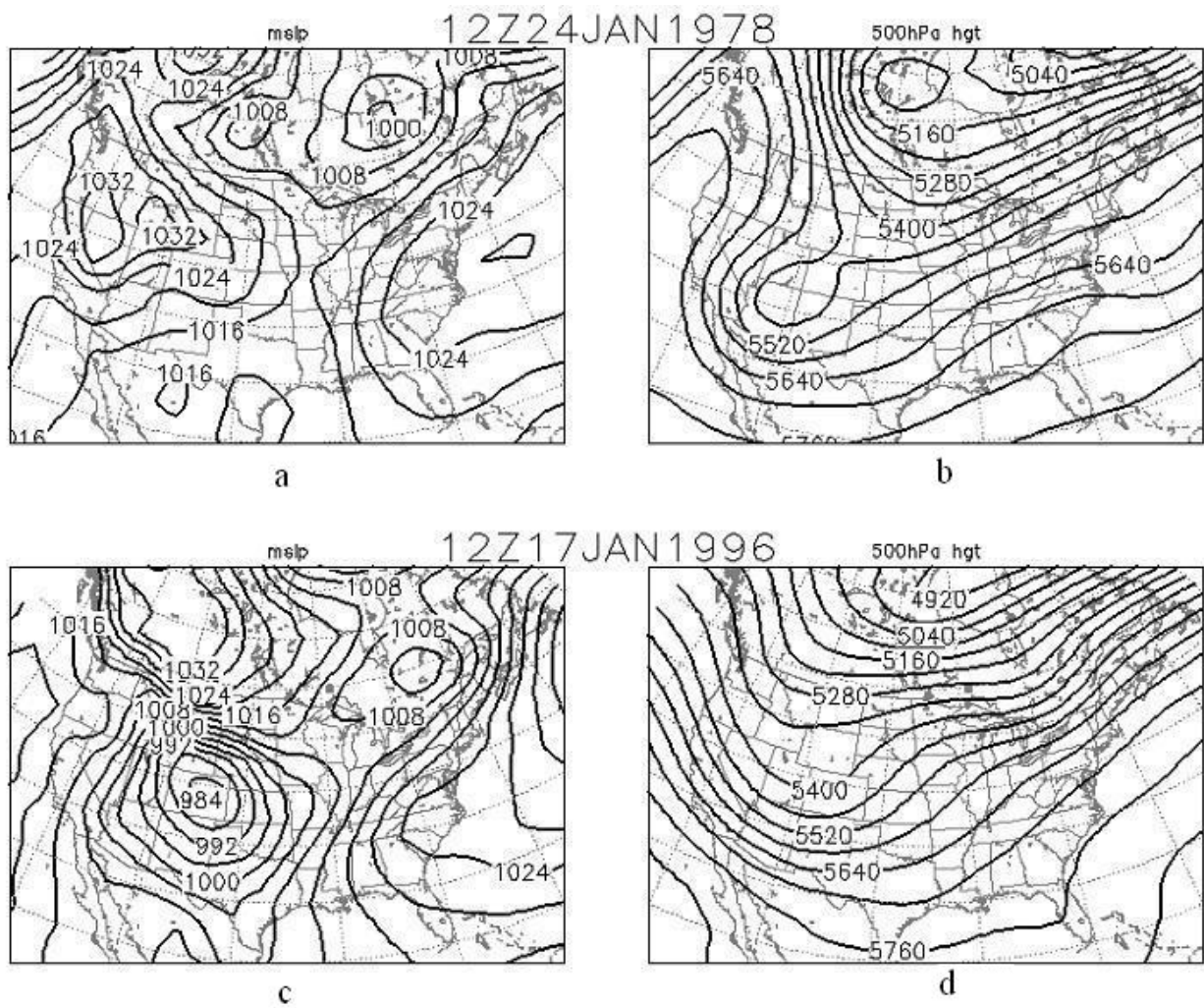


Figure 9. Mean sea level pressure (hPa) and 500 hPa heights (meters) at 12 UTC 24 January 1978 (a,b) and 12 UTC 17 January 1996 (c,d).

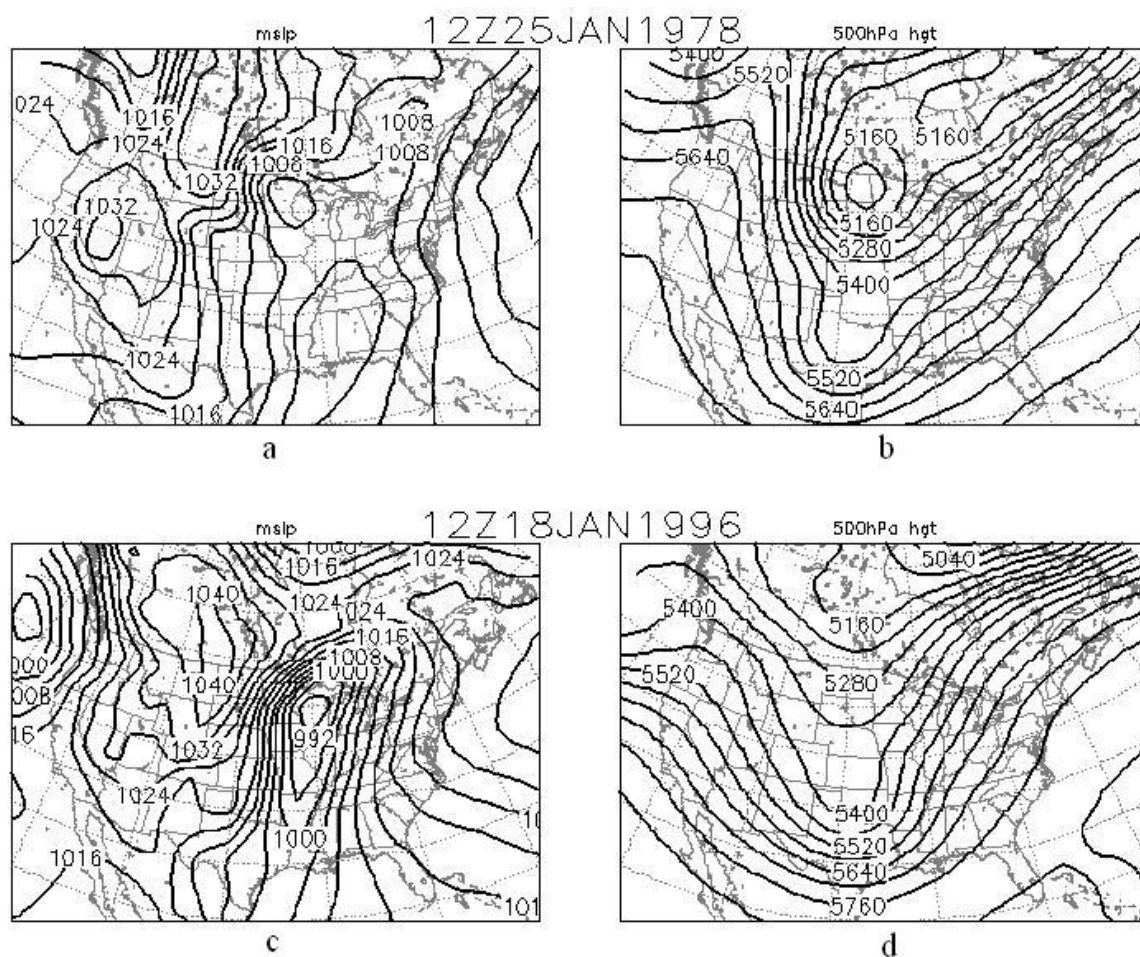


Figure 10. Mean sea level pressure (hPa) and 500 hPa heights (meters) at 12 UTC 25 January 1978 (a,b) and 12 UTC 18 January 1996 (c,d).

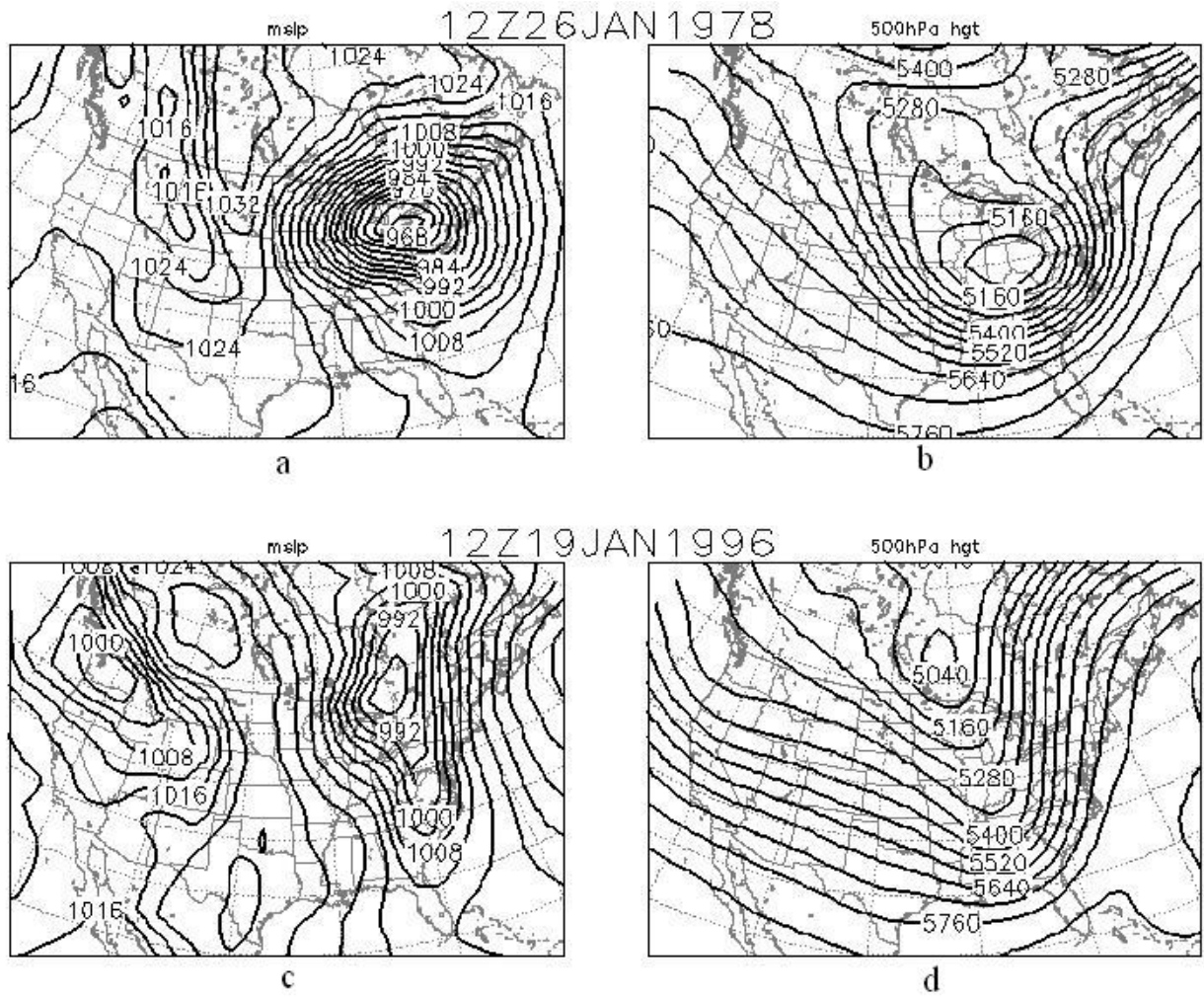


Figure 11. Mean sea level pressure (hPa) and 500 hPa heights (meters) at 12 UTC 26 January 1978 (a,b) and 12 UTC 19 January 1996 (c,d).

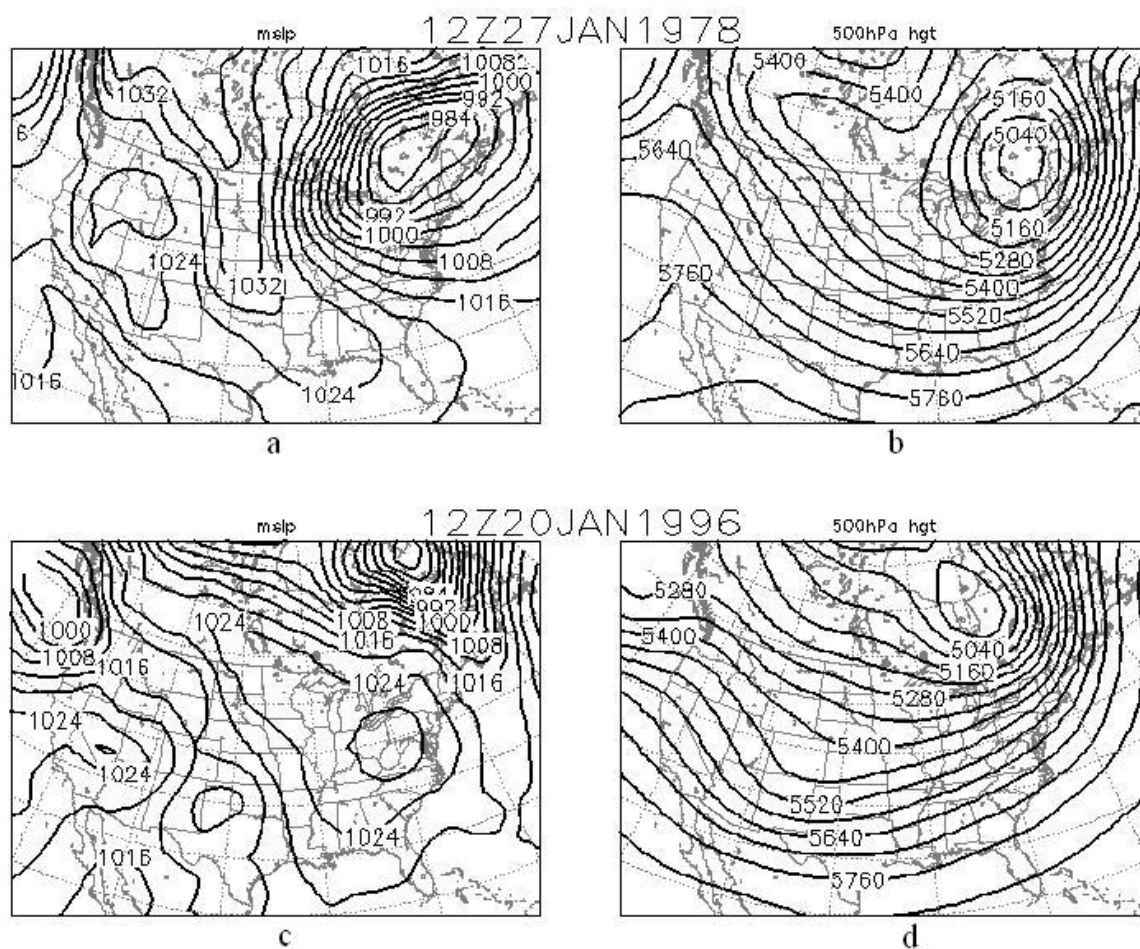


Figure 12. Mean sea level pressure (hPa) and 500 hPa heights (meters) at 12 UTC 27 January 1978 (a,b) and 12 UTC 20 January 1996 (c,d).

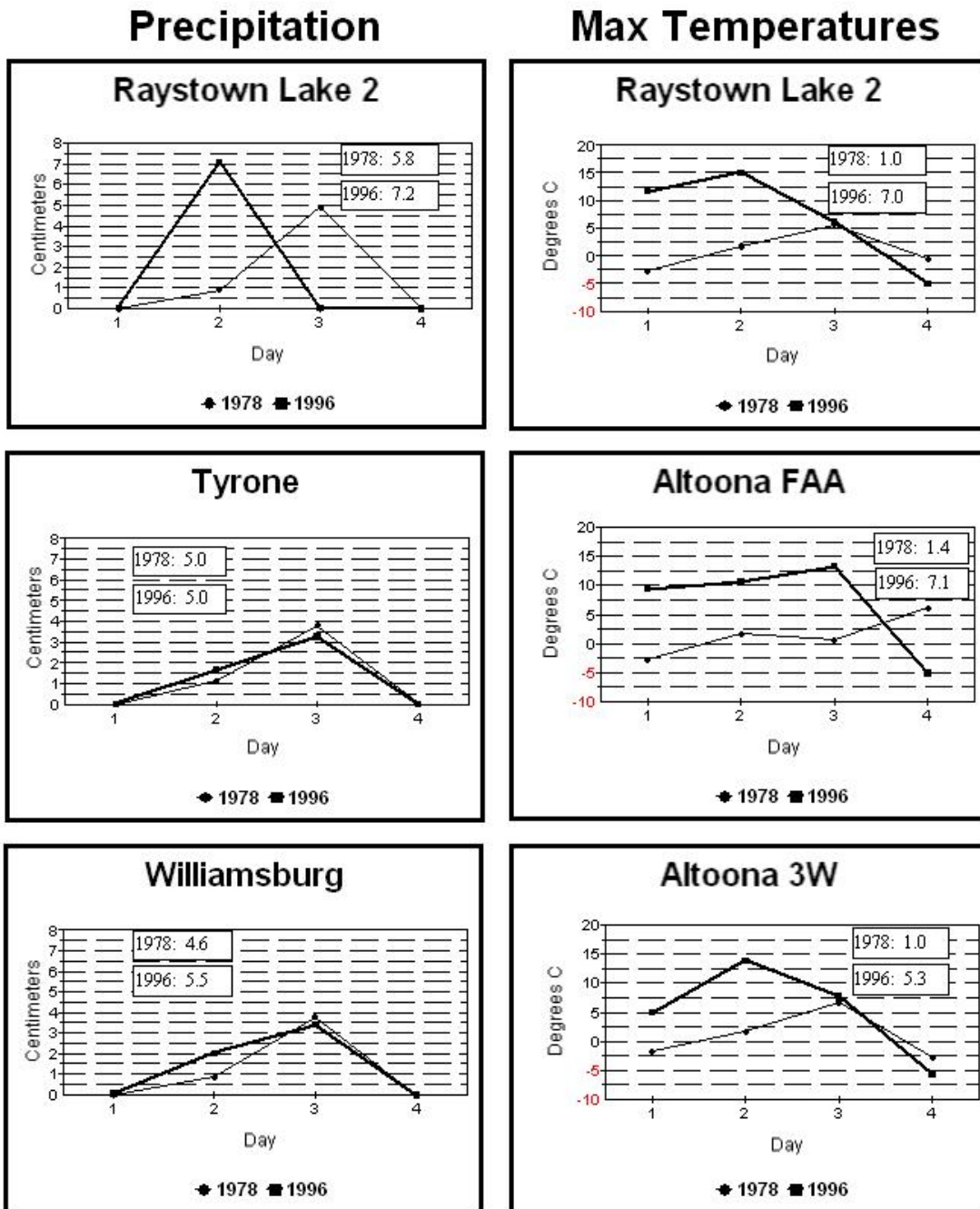


Figure 13. Observed daily precipitation (cm) and observed daily maximum temperatures (°C) for 24-27 January 1978 (thin traces) and 18-21 January 1996 (thick traces) for select stations in and near the study area. Event total precipitation and event average maximum temperatures are also indicated.

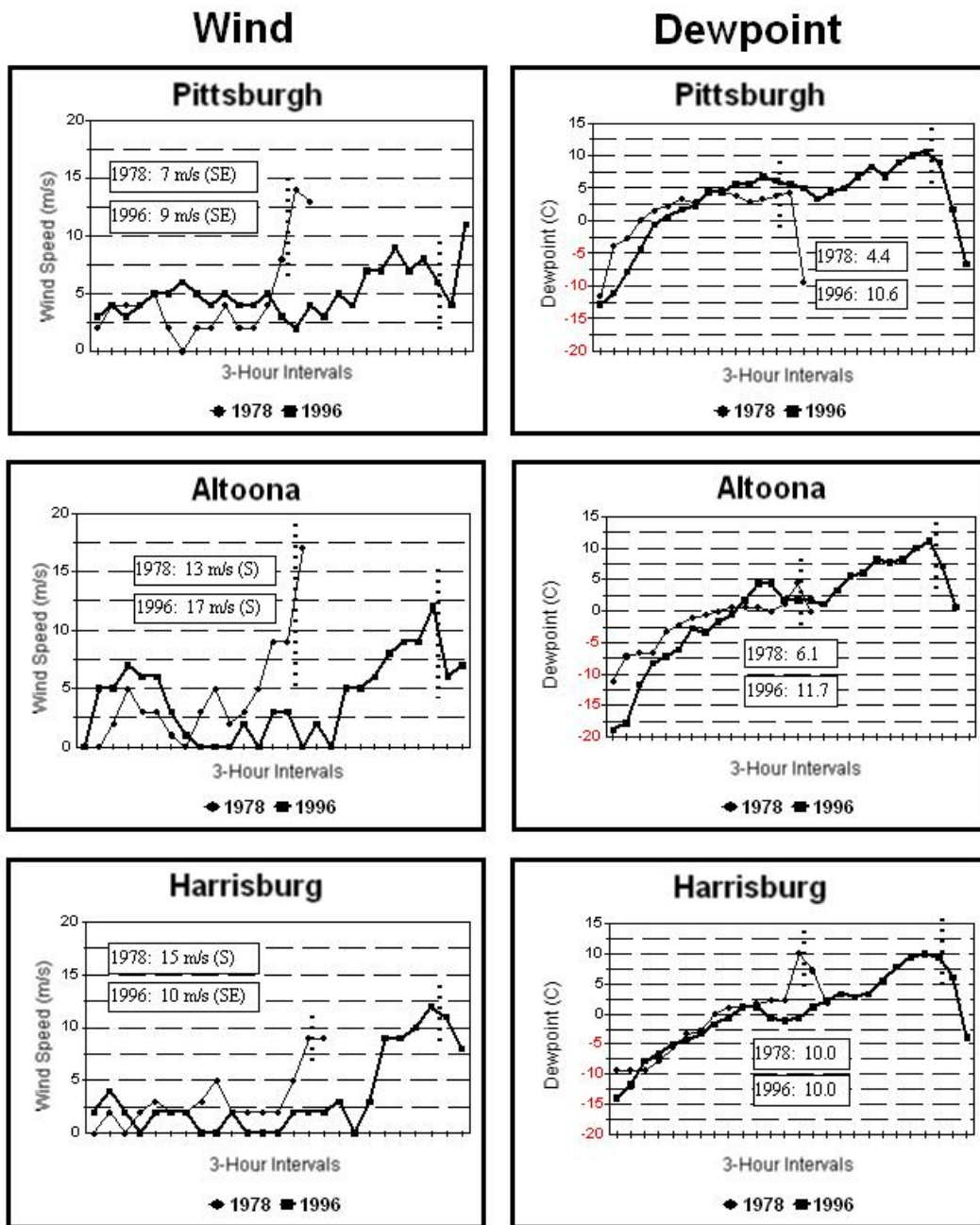


Figure 14. Observed three-hourly wind speeds (m s^{-1}) and observed surface dewpoint temperatures ($^{\circ}\text{C}$) during the J78 (thin traces) and J96 (thick traces) events for select stations in and near the study area. The fastest wind speeds (m s^{-1}) and directions are also indicated, as are the maximum observed dewpoint temperatures ($^{\circ}\text{C}$). Vertical (dashed) lines indicate cold frontal passages. Note that no times are provided along the x-axis. Each trace begins when wind direction data (not shown) and dewpoint temperature data associated with each of the two events first indicated that warm air advection had begun at the specified location.

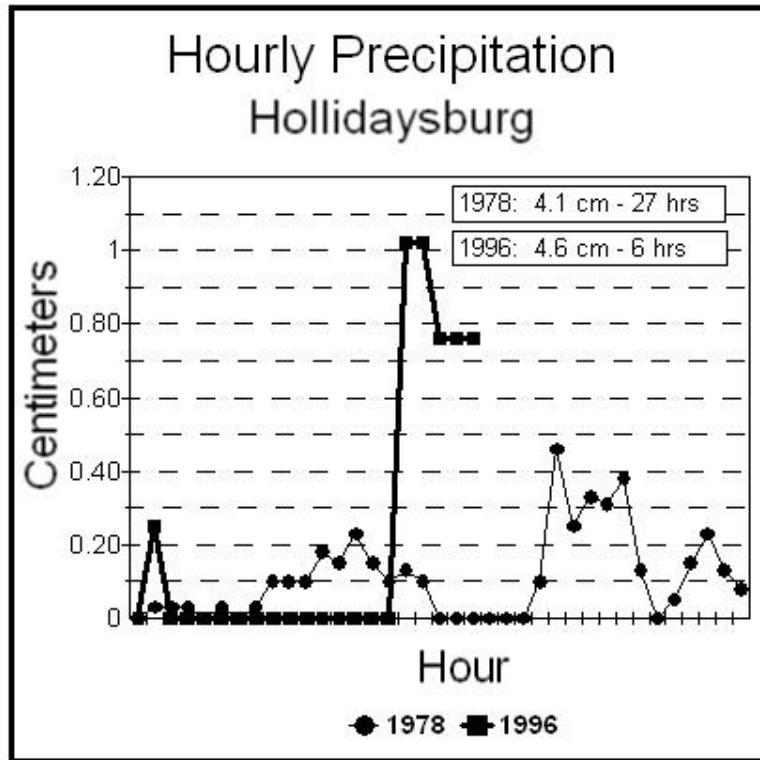


Figure 15. Observed hourly precipitation (cm) during the J78 (thin trace) and J96 (thick trace) events at Hollidaysburg, PA. Event total precipitation (cm) and total number of hours with precipitation reported are also indicated. Note that each trace ends with the last report of measurable precipitation in association with the event.

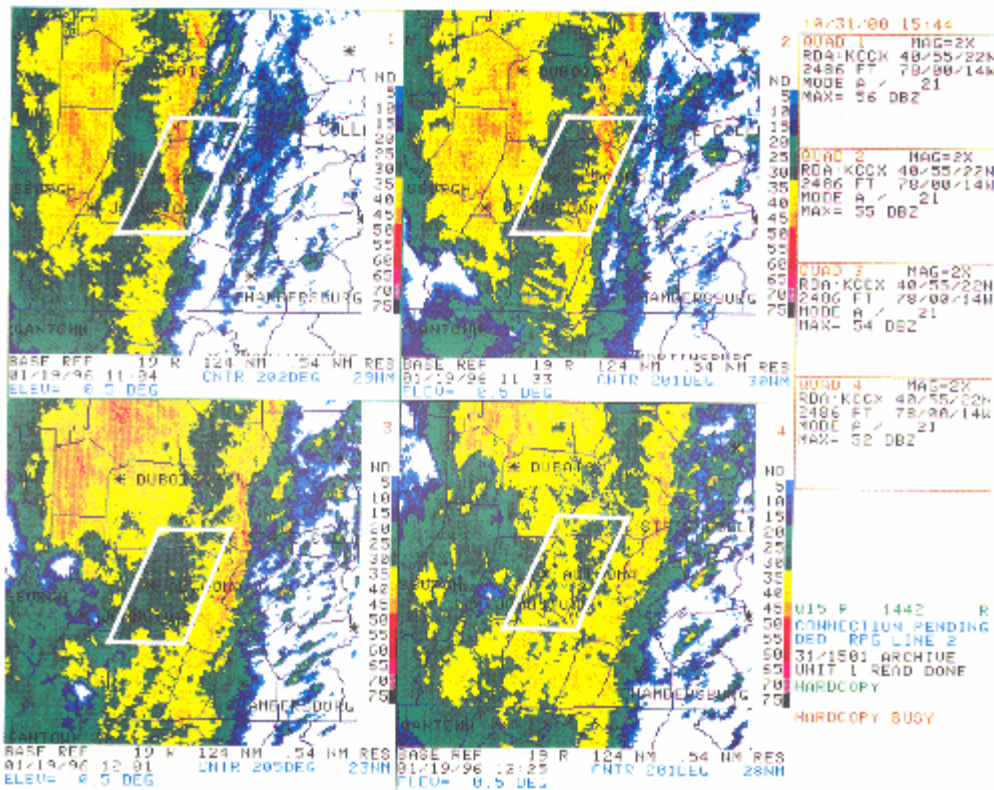


Figure 16. State College, PA WSR-88D reflectivity (dBZ) images at 1104, 1133, 1201, and 1225 UTC 19 January 1996 (top row, left to right, then bottom row, left to right). The study area is located within the white parallelogram.

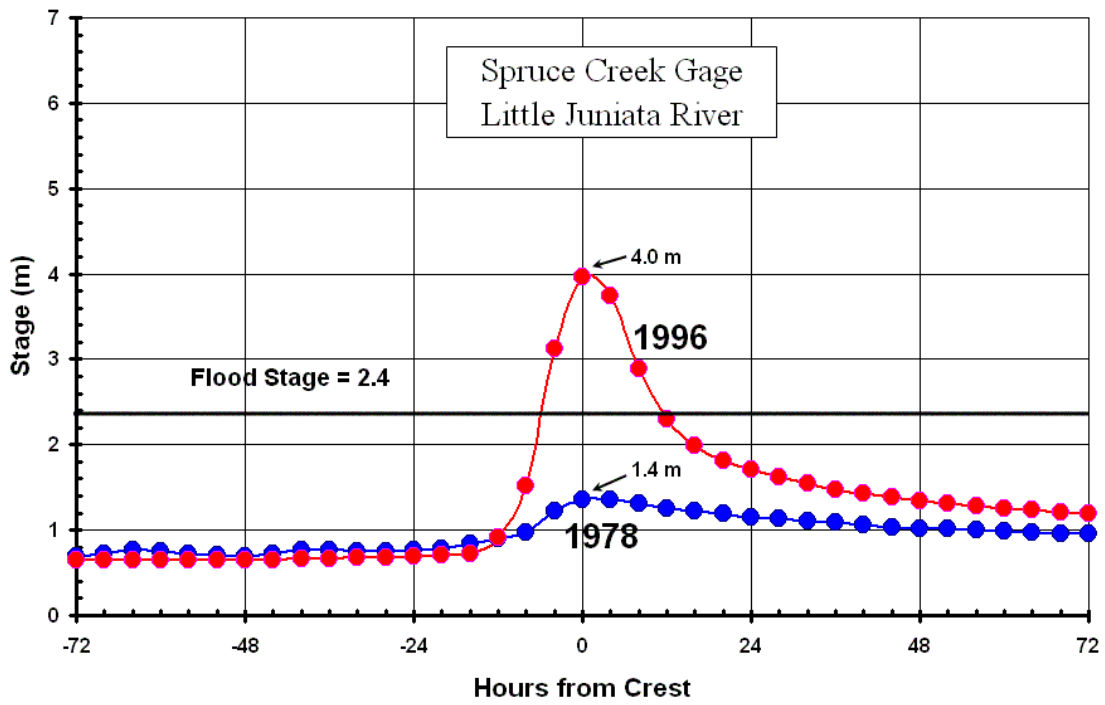


Figure 17. Comparison of the hydrologic response (meters) at the Spruce Creek, Little Juniata River, stream gage (refer to Fig. 2) that resulted from the J78 (blue trace) and J96 (red trace) catalyst meteorological events. Flood stages are also indicated (meters).

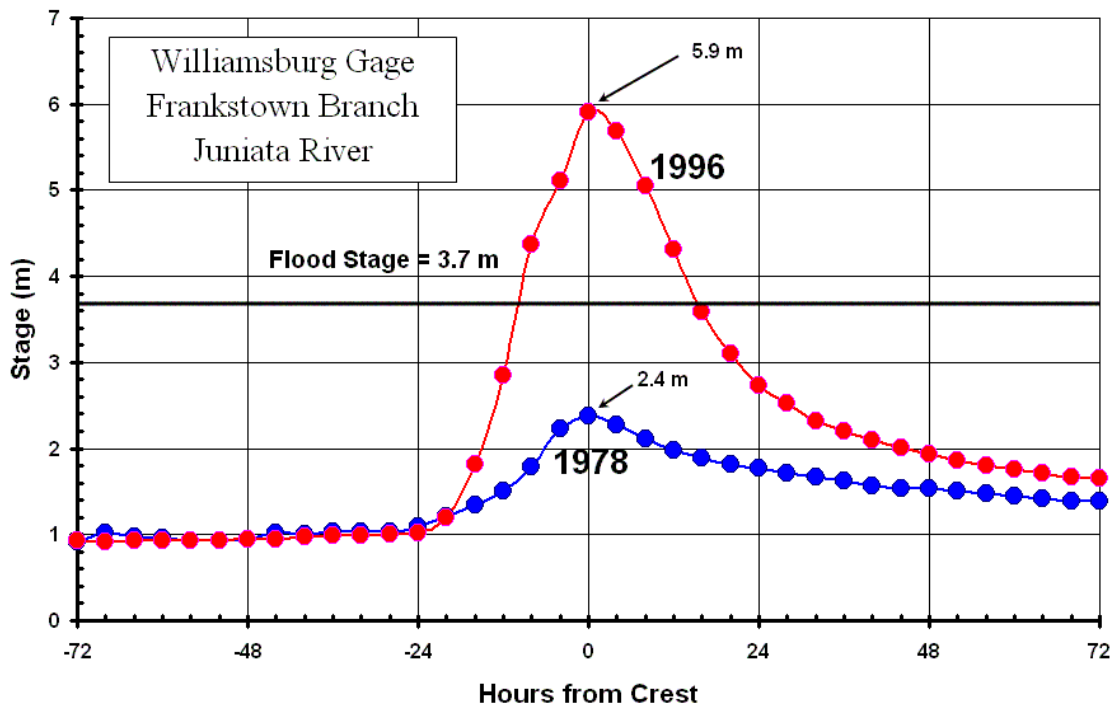


Figure 18. Comparison of the hydrologic response (meters) at the Williamsburg, Frankstown Branch Juniata River, stream gage (refer to Fig. 2) that resulted from the J78 (blue trace) and J96 (red trace) catalyst meteorological events. Flood stages are also indicated (meters).

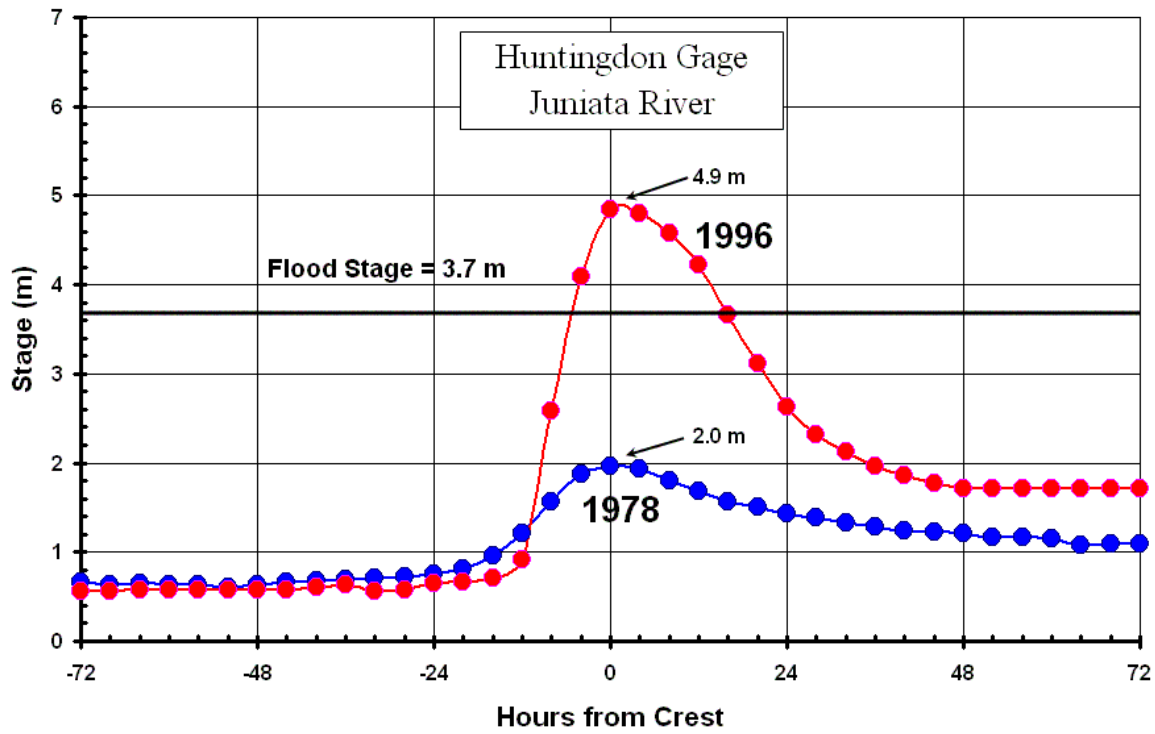


Figure 19. Comparison of the hydrologic response (meters) at the Huntington, Juniata River, stream gage (refer to Fig. 2) that resulted from the J78 (blue trace) and J96 (red trace) catalyst meteorological events. Flood stages are also indicated (meters).

TABLES

Table 1. Comparison of NWS SNOW-17 model output for the J78 (top) and the J96 (bottom) events at the Huntingdon, PA stream gage.

SNOW-17 Output							
<i>January 1978 – Juniata River at Huntingdon</i>							
<u>Day</u>	<u>Snowfall</u>	<u>Rainfall</u>	<u>Energy Exchange</u>	<u>Sim. Areal Coverage</u>	<u>Pct. Liquid Water</u>	<u>Heat Deficit</u>	<u>Sim. Water Equivalent</u>
20	1.10	0.00	-.07	.99	.1	.21	3.43
21	0.04	0.00	-.02	.99	.1	.23	3.46
22	0.00	0.00	-.04	.98	.1	.27	3.44
23	0.00	0.00	.00	.96	.1	.27	3.43
24	0.05	0.10	.11	1.00	.1	.06	3.57
25	0.00	1.05	.27	.86	16.0	.00	4.03
26	0.00	0.59	-.08	.84	16.0	.09	3.86
27	0.02	0.00	-.06	.84	15.9	.15	3.86
<i>January 1996 – Juniata river at Huntingdon</i>							
<u>Day</u>	<u>Snowfall</u>	<u>Rainfall</u>	<u>Energy Exchange</u>	<u>Sim. Areal Coverage</u>	<u>Pct. Liquid Water</u>	<u>Heat Deficit</u>	<u>Sim. Water Equivalent</u>
15	0.00	0.00	.28	1.00	1.6	.00	3.56
16	0.00	0.00	.02	1.00	13.6	.03	3.56
17	0.02	0.01	.03	1.00	13.6	.00	3.57
18	0.00	0.01	.21	1.00	20.0	.00	3.56
19	0.00	0.71	.88	.87	20.0	.00	2.62
20	0.00	1.35	.18	.86	20.0	.05	2.18
21	0.00	0.00	-.02	.80	20.0	.07	2.17
22	0.00	0.00	-.00	.80	20.0	.17	2.17